ACS EARTH AND SPACE CHEMISTRY

Article

Cite This: ACS Earth Space Chem. 2018, 2, 1196−1210

http://pubs.acs.org/journal/aesccq

Functional Group Composition of Secondary Organic Aerosol Formed from Ozonolysis of α-Pinene Under High VOC and Autoxidation Conditions

Megan S. Claflin,[†,‡] Jordan E. Krechmer,[†,‡,§] Weiwei Hu,[†,‡,∥] Jose L. Jimenez,[†,‡] and Paul J. Ziemann*[,†,‡]

[†]Cooperative Institute for Research in Environmental Sciences (CIRES), Boulder, Colorado 80309, United States

[‡]Department of Chemistry and Biochemistry, University of Colorado, Boulder, Colorado 80309, United States

Supporting Information

ABSTRACT: The formation of secondary organic aerosol (SOA) from α-pinene ozonolysis has been widely studied, with a recent focus on contributions from highly oxidized multifunctional compounds (HOMs) that have been observed in laboratory and field studies. Most of what is known about the chemical composition of SOA and HOMs, however, consists of molecular formulas and limited molecular structure identification based on mass spectrometric analysis. Here, we characterized the SOA formed from α-pinene ozonolysis using derivatization-spectrophotometric methods to quantify peroxide, carbonyl, carboxyl, ester, and hydroxyl groups. Experiments were conducted over a range of α-pinene concentrations and relative humidities, including regimes in which gas-phase HOMs were detected using NO_3^- chemical ionization mass spectrometry. Results for experiments conducted with high concentrations of α-pinene were also compared with predictions of a model that employed the Master Chemical Mechanism and included gas-particle and gas-wall partitioning. It appears that gas-phase monomer and dimer products formed through $RO_2^\bullet$ + $RO_2^\bullet$, $RO_2^\bullet$ + HO_2, $RO_2^\bullet$ isomerization, and stabilized Criegee intermediate + carboxylic acid or water reactions contributed to SOA formation, but that in particles the aldehyde and ketone groups in these compounds were often converted to carboxyl and ester groups through Baeyer−Villiger reactions with hydroperoxides and peroxycarboxylic acids. Evidence also indicates that hydrolysis of dimers containing diacyl peroxide groups contributed to the formation of carboxyl and ester groups, that hydroxyl groups were less abundant in SOA than expected (because of minor gas-phase alkoxy radical isomerization or conversion to an undetectable acetal oligomer), and that gas-to-particle partitioning of small carbonyl compounds may have contributed to SOA.

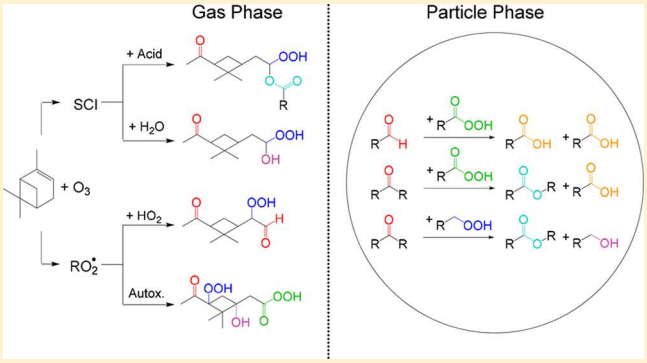

KEYWORDS: *monoterpene oxidation, ozonolysis, multiphase chemistry, Baeyer−Villiger reactions, oligomers, highly oxidized multifunctional compounds*

INTRODUCTION

According to global estimates approximately 1000 Tg of nonmethane volatile organic compounds (VOCs) are emitted into the atmosphere each year, with biogenic VOCs accounting for more than two-thirds of the emissions.[1] These VOCs can react with OH radicals, NO_3 radicals, and O_3 to form oxygenated products that can either remain in the gas phase or participate in secondary organic aerosol (SOA) growth.[2] This SOA material contributes significantly to the mass of atmospheric fine particles[3] and has the potential to impact regional and global air quality, climate, and human health.[4] The oxidation of monoterpenes, which comprise ∼15% of biogenic VOCs,[1] has been estimated to account for a substantial fraction of the global SOA budget.[5] As a result, numerous laboratory and modeling studies have been conducted to better understand the products and mechanisms of these reactions and the chemical and physical properties of the SOA that is formed.[5−10] Many of these studies have focused on the dominant monoterpene, α-pinene, which accounts for over 40% of global monoterpene emissions.[1] α-Pinene ozonolysis has received the most attention since this reaction is the major atmospheric sink for α-pinene[11] and forms SOA in large yields.[5,12,13] Laboratory studies of this reaction have identified and quantified a number of gas- and particle-phase products,[5,6,8,10] and models such as the Master Chemical Mechanism (MCM)[7] and Biogenic hydrocarbon Oxidation and Related Aerosol formation Model (BOREAM)[9]

Received: August 22, 2018
Revised: October 8, 2018
Accepted: October 10, 2018
Published: October 10, 2018

DOI: 10.1021/acsearthspacechem.8b00117
ACS Earth Space Chem. 2018, 2, 1196−1210

have been used to simulate the reactions that lead to SOA formation for comparison with measurements of SOA yields and molecular composition. Because of this large body of work, and in spite of the chemical complexity and general lack of knowledge of the composition of the SOA formed from α-pinene ozonolysis, this material has to a large extent become the de facto "standard SOA" for the aerosol community.

More recently, α-pinene ozonolysis has returned to the forefront of SOA research because of the detection of highly oxygenated multifunctional compounds (HOMs) among its gas-phase products and the demonstrated significance of these to new particle formation and growth, particularly in pristine, forested areas.[14−18] In 2012, Ehn et al.[14] first reported elemental formulas for HOMs and demonstrated the use of nitrate ion chemical ionization mass spectrometry (NO_3^- CIMS) as an effective method for HOM detection. In a later study of α-pinene ozonolysis, Ehn et al.[15] detected HOMs in the gas-phase with O/C atomic ratios >0.7, with corresponding HOM aerosol mass yields of 14−18%, and attributed the observed rapid formation of HOMs to autoxidation reactions in which organic peroxy radicals ($RO_2^•$) are propagated by intramolecular H-shifts that rapidly add functional groups to the molecule. The proposed role of autoxidation in HOM formation has been supported by other experimental studies as well as quantum chemical calculations that have been used to develop detailed mechanisms of HOM formation from ozonolysis of a variety of biogenic VOCs and other cyclic alkenes.[16,19] There remains considerable uncertainty surrounding these mechanisms, however, since theory has shown that proposed $RO_2^•$ isomerization reactions would be too slow to explain the observed rates of HOM formation from α-pinene ozonolysis because of constraints imposed by the bicyclic structure of the parent VOC.[20] Nonetheless, these studies have provided useful guidelines in attempts to develop gas-phase mechanisms of HOM formation.[16,19] Other studies have focused on the fate of HOMs in aerosol particles[17,21] since they are thought to contain functional groups including peroxycarboxyl, hydroperoxide, carbonyl, and hydroxyl,[16,19,21] all of which make HOMs vulnerable to particle-phase reactions.[2,13] For example, Mutzel et al.[17] investigated the effects of seed particle composition on the composition of SOA formed from α-pinene ozonolysis under conditions in which gas-phase HOMs were present. They observed carboxylic acids and short-chain carbonyls, presumably formed through decomposition of ketohydroperoxides, as well as intact HOMs, all in the particle phase. In experiments conducted under similar conditions, Krapf et al.[21] observed significant loss of peroxides from SOA and associated decreases in SOA mass and increases in SOA oxidation state on time scales of tens of minutes.

Although considerable progress has been made in determining the products and mechanism of α-pinene ozonolysis and in identifying reactions that may lead to the formation of HOMs and SOA, detailed information on the chemical constituents, reactions, and processes that determine the composition of this SOA is still very limited. In light of these deficiencies, we have conducted a series of environmental chamber experiments to investigate the effects of VOC concentration, relative humidity (RH), and particle-phase reactions on the functional group composition of SOA formed from α-pinene ozonolysis over a range of conditions, including those that have been employed previously for studies of HOM formation. The study employs methods we have recently developed for quantifying the contributions of peroxide, ester, carbonyl, carboxyl, and hydroxyl groups to SOA formed at high[22] and low[23] VOC concentrations, which helps to constrain currently available gas-phase, autoxidation, and particle-phase reaction products and mechanisms, as well as proposed molecular structures of HOMs.

EXPERIMENTAL SECTION

Chemicals. The following chemicals, with purities/grades and suppliers were used: (1*S*)-(−)-α-pinene (99%), tridecanoic acid (98%), 1,2-tetradecanediol (90%), benzoyl peroxide (98%), cyclohexane (99%, ACS grade) (Sigma-Aldrich); bis(2-ethylhexyl) sebecate (97%) (Fluka); 3-hexadecanone (99%) (ChemSampCo); ethyl acetate (99.5%) (EMD Millipore); 18 MΩ water purified using Milli-Q Advantage A10 water system. O_3 was generated using a BMT 802N O_3 generator with ultrahigh purity (UHP) O_2 (Airgas). Chemicals used for functional group analyses have been reported previously.[13,22,23]

Environmental Chamber Experiments. Two sets of α-pinene ozonolysis experiments were conducted: a set of low-VOC concentration experiments (Low-VOC) and a set of high-VOC concentration experiments (High-VOC). The Low-VOC experiments were conducted with 10 ppb α-pinene and 300 ppb O_3 in dry (<1% RH) and humid (65% RH) air, whereas the High-VOC experiments were conducted with 1 ppm α-pinene and 2 ppm of O_3 in dry (<1% RH) and humid (50% and 85% RH) air. The Low-VOC experiments were conducted in one of two 20 m^3 Teflon FEP chambers that are part of the recently constructed CU Chamber facility. These two chambers are fully and separately enclosed with computer-regulated temperature and RH controls. The High-VOC experiments were conducted in an 8.0 m^3 Teflon FEP chamber at room temperature (∼25 °C) and pressure (∼630 Torr for Boulder, CO). Both chambers were filled and flushed with clean, dry air (<5 ppb hydrocarbons, <1% RH) from AADCO clean air generators. Chemicals were added to the chamber by evaporation from a heated glass bulb into a stream of UHP N_2, and a Teflon-coated fan was run for ∼1 min after each addition to mix the chemicals. Water was added to adjust the RH when needed, and no seed aerosol was used in the experiments. For the Low-VOC experiments, 100 ppb of cyclohexane was added as an OH scavenger and then 300 ppb of O_3 followed by 10 ppb of α-pinene to initiate the reaction. Using a simple kinetic model and published rate constants, it was estimated that ∼80% of the α-pinene reacted with O_3 and ∼20% with OH radicals and that only ∼5% of the first-generation products reacted further with OH radicals.[9,24−27] For the High-VOC experiments, 1200 ppm of cyclohexane (sufficient to scavenge >99% of the OH radicals formed during the reaction)[13] was added and then 1 ppm of α-pinene followed by 2 ppm of O_3 to initiate the reaction.

Gas Analysis. Highly oxidized gas-phase reaction products were detected in the Low-VOC experiments using an Aerodyne high-resolution time-of-flight mass spectrometer employing a nitrate-ion chemical ionization source (NO_3^- CIMS). The instrument, source, and experimental configuration have been described in previous publications.[28−31] The NO_3^-CIMS was placed inside the environmental chamber enclosure so that only a 0.7 m × 15 mm inner diameter electropolished stainless steel inlet was needed to continuously sample 10 standard L min^{-1} of air. This inlet helped reduce the loss of HOMs to the inlet walls (estimated ∼70% trans-

DOI: 10.1021/acsearthspacechem.8b00117
ACS Earth Space Chem. 2018, 2, 1196−1210

mission). The O_3 concentration was monitored during the reaction using a Thermo Scientific 49i O_3 monitor.

Particle Analysis. Particle size distributions and volume concentrations were measured during each experiment using a TSI model 3080 scanning mobility particle sizer (SMPS) with a TSI model 3775 condensation particle counter. Submicron nonrefractory organic aerosol (OA) was measured using an Aerodyne High Resolution Time-of-Flight Aerosol Mass Spectrometer (HR-ToF-AMS)[32] with a newly designed capture vaporizer.[33,34] Elemental O/C and H/C atomic ratios of total OA were calculated according to the laboratory calibration for a standard vaporizer.[35,36] Differences between the standard and capture vaporizers were accounted for using results from a comparison of measurements made with collocated AMSs with both vaporizers during the 2013 SOAS field study, which was dominated by biogenic SOA.[37−40] The uncertainty of elemental ratios is estimated as ±28% for O/C and ±14% for H/C.[36]

Two replicate SOA samples were collected after each experiment onto preweighed filters (Millipore Fluoropore PTFE, 0.45 μm) for 120 min at a flow rate of 14 L min^{-1}. Immediately after sampling, the filters were reweighed to determine the mass of SOA collected. Filters were weighed to ±0.5 μg using a Mettler Toledo XS3DU Microbalance. Filter samples were extracted twice into 5 mL of ethyl acetate within 10 min after sampling. Extracts were then combined in a preweighed vial and dried in a stream of UHP N_2, and the vial was reweighed to determine the extracted SOA mass. Comparison of collected and extracted SOA masses indicated extraction efficiencies were >95%. The dried SOA was reconstituted in ethyl acetate to achieve a sample concentration of 1 μg μL^{-1} for subsequent functional group analysis and stored at −20 °C between analyses. SOA functional group composition was quantified using the micromethods described by Ranney and Ziemann[23] for the Low-VOC experiments and using the macro-methods described by Aimanant and Ziemann[22] and Docherty et al.[13] for the High-VOC experiments. These two methods differ primarily in the amounts of reagents and sample used and have been previously compared for standards and SOA and give similar results.[23] Benzoyl peroxide, bis(2-ethylhexyl) sebacate, 3-hexadecanone, tridecanoic acid, and 1,2-tetradecanediol were employed as surrogate standards for peroxide, ester, carbonyl, carboxyl, and hydroxyl groups, respectively.

The SOA mass yield was quantified as the mass of SOA formed divided by the mass of α-pinene reacted. The mass of SOA formed was calculated from the filter mass measurements with corrections for particle wall loss during the 2 h sampling period using SMPS measurements and the method described in Yeh et al.[41] Because of the concentrations of O_3 used in these experiments and the large excess relative to α-pinene, the lifetime of α-pinene was sufficiently short (about 5 and 25 min for the High-VOC and Low-VOC experiments) so that essentially all α-pinene reacted prior to filter sampling. For this reason, the concentration of α-pinene reacted was assumed to be equal to the initial added concentration.

No attempt was made to correct measured SOA yields for loss of gas-phase products to the chamber walls[30,42] (which has only been done a few times by conducting experiments with increasing amounts of seed particles[43,44]), but such losses were included in the modeling conducted for the High-VOC experiments in order to improve the validity of the comparison of the model predictions with measurements. These losses had no significant effect on the predicted composition of the SOA (typically less than ∼10% for any value) compared to when they were not included and so probably had a similarly minor effect on the measured SOA composition and yields. This was because most semivolatile products partitioned to the large mass of SOA that was present before they could partition to the walls.[31] Such losses may have been significant in the Low-VOC experiments where SOA mass concentrations were small, but no modeling was conducted for those experiments (for reasons described below) that could have provided estimates of these losses.

Description of Functional Group Composition and Other Properties of SOA. The functional group composition of SOA was expressed as the average number of each measured functional group per parent VOC molecule,[22] assuming that the SOA contained only peroxide [CHOOH], ester [C(O)O], carbonyl [C(O)], carboxyl [C(O)OH], hydroxyl [CHOH], and methylene [CH_2] groups. This composition was determined by first summing the masses of measured functional groups, calculated as the measured moles × molecular weight (g mol^{-1}) of each group: peroxide = 46, ester = 44, carbonyl = 28, carboxyl = 45, hydroxyl = 30. The moles of methylene groups were then obtained by subtracting this sum from the measured SOA mass and dividing by 14, the molecular weight of CH_2. Molar concentrations of functional groups were used to calculate mole fractions, which were then multiplied by 10, the carbon number of α-pinene, to obtain the number of functional groups per C_{10} molecule in SOA.

The uncertainties in the functional group measurements were estimated as standard deviations calculated from analyses conducted for each of four replicate dry (0% RH) Low-VOC experiments, three replicate humid (65% RH) Low-VOC experiments, and the single experiments conducted for each of the High-VOC conditions (0%, 50%, and 85% RH), where two replicate samples from each experiment were analyzed. In addition, there are inherent uncertainties in the analyses that stem from differences in the molar absorptivity of derivatized SOA compounds and the surrogate standards used for quantification. Previous studies conducted with a large variety of monofunctional and multifunctional compounds indicate that these uncertainties are approximately (±) 10%, 30%, 10%, 20%, and 20% for peroxide, ester, carbonyl, carboxyl, and hydroxyl groups.[22,45]

The measured functional group composition was used to calculate the O/C and H/C ratios, molecular weight, and the saturation concentration of the SOA, with the latter calculation employing SIMPOL.1[46] to estimate effects of functional groups on compound vapor pressure. The density of the SOA was estimated using O/C and H/C ratios and the parametrization of Kuwata et al.[47] The SOA molar yield (moles of SOA formed/mol of α-pinene reacted) was calculated by dividing the SOA mass yield (mass of SOA formed/mass of α-pinene reacted) by the molecular weight of the SOA.

Modeling Functional Group Composition and Other SOA Properties. Our experimental results for the High-VOC experiments were compared with results of simulations conducted using the Master Chemical Mechanism (MCM, http://mcm.leeds.ac.uk/MCM),[48,49] which is a detailed gas-phase chemical mechanism that can be used to model the kinetics of complex oxidation reactions of volatile organic compounds and to estimate reaction products and their yields. The MCM is widely used for atmospheric chemistry modeling.

DOI: 10.1021/acsearthspacechem.8b00117
ACS Earth Space Chem. 2018, 2, 1196−1210

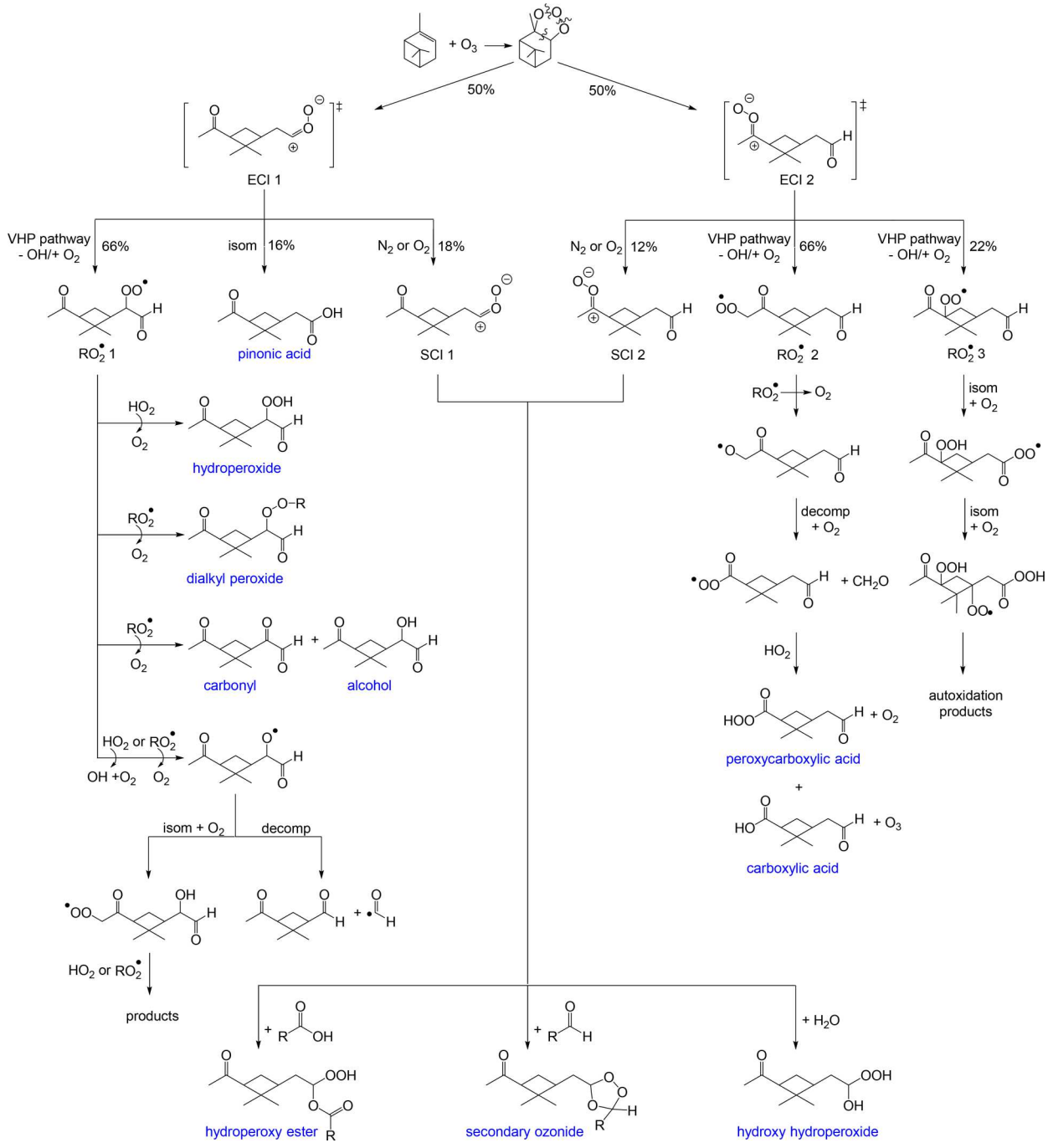

Figure 1. Formation mechanism of the SCI and $RO_2^\bullet$ radicals from the ozonolysis of α-pinene. Only syn ECI and SCI isomers are shown, and labeled branching ratios are from Capouet et al.[9] The generation of the different functional groups are shown through subsequent reactions of the SCI and $RO_2^\bullet$ radicals.

The MCM was not used to simulate the results of the Low-VOC experiments since it does not include autoxidation reactions that are expected to have major effects on the SOA composition due to the lower $RO_2^\bullet$ radical and SOA mass concentrations. The model predicts an array of gas-phase products that contain hydroperoxide, peroxycarboxyl, carbonyl, carboxyl, ester, and hydroxyl groups. While all products produced in the model were tracked, only products that had molar yields above 1% were used to estimate SOA composition. These compounds accounted for 96% of the total carbon reacted in the modeled High-VOC reactions.

We note that one modification was made to the model with regard to the fate of stabilized Criegee intermediates (SCI). In the MCM, it is always assumed that SCI react with water vapor (their most common fate in the atmosphere) to form hydroxy hydroperoxides that then decomposes to pinonaldehyde or pinonic acid, even though under dry conditions SCI will react with aldehydes to form secondary ozonides and with carboxylic acids to form hydroperoxy esters.[25,50] The major small aldehydes formed in the ozonolysis of α-pinene are formaldehyde and acetaldehyde, and the major small carboxylic acids are formic and acetic acid, with reported measured molar yields of 30%, 3%, 8%, and 8%, respectively.[8] In addition, the

DOI: 10.1021/acsearthspacechem.8b00117
ACS Earth Space Chem. 2018, 2, 1196−1210

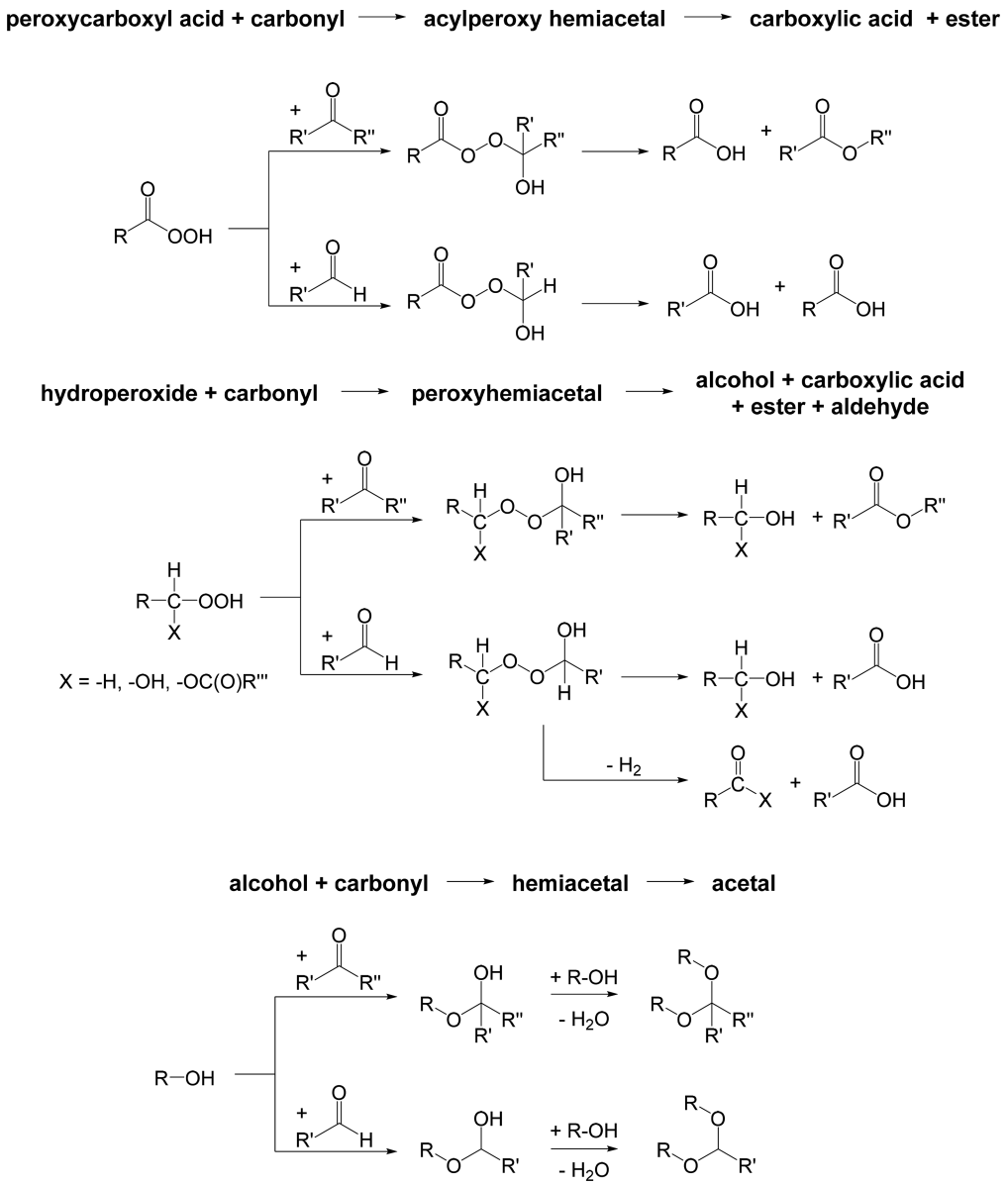

Figure 2. Particle-phase reactions of peroxycarboxyl, hydroperoxy, and hydroxyl groups with aldehydes and ketones resulting in the formation of carboxyl, ester, and hydroxyl groups along with acylperoxy hemiacetal, peroxyhemiacetal, hemiacetal, and acetal oligomers.

MCM predicts that under High-VOC conditions pinonic acid, pinic acid, hydroxy pinonic acid, and a C_9 aldo-acid are formed with molar yields of 10%, 3%, 2%, and 6%. These larger carboxylic acids are important for modeling the fate of SCI in the dry High-VOC reaction since it has been shown that large carboxylic acids (heptanoic acid) react ∼2.5 times faster than small carboxylic acids (formic acid) and ∼6 times faster than small aldehydes (formaldehyde).[50] In our modeling the yields given above were used with relative rate constants for reactions of SCI[50] to estimate the yields of products formed in the dry reaction, whereas under humid conditions the SCI were assumed to react with water vapor to form hydroxy hydroperoxides that did not decompose to pinonaldehyde and water, consistent with our previous studies of these types of compounds.[51] The $RO_2^{\bullet}$ + HO_2 reaction is the only other gas-phase reaction that is known to be affected by humidity, and although the dependence is not included in the MCM, the effect should be small since at 50% RH the rate constant is only 1.5 times larger.[52] We also added the "hot-acid" decomposition of ECI for both dry and humid conditions, which has been shown to result in an ∼8% yield of pinonic acid[9] but is not included in the MCM.

The concentrations of all gas-phase products were calculated at 10 s intervals for 10 min of reaction, at which time all the α-pinene had reacted and product concentrations were constant. The concentrations of all products in the gas- and particle-phases and the chamber walls were then calculated for the following 2 h filter sampling period at 10 s intervals starting with the values at 10 min and using an iterative procedure similar to that described by Colville and Griffin[53] in which the fraction of each compound that partitioned into the particles and walls was estimated using gas-particle[54] and gas-wall[42] partitioning theories. For gas-particle partitioning calculations, equilibrium was assumed to be achieved instantly at each time interval (which is valid for these high SOA mass concentrations[42]), compound vapor pressures were estimated using the SIMPOL.1 group contribution method,[46] particle-phase activity coefficients were assumed to be unity, and the SOA

DOI: 10.1021/acsearthspacechem.8b00117
ACS Earth Space Chem. 2018, 2, 1196−1210

mass concentration into which products partitioned was parametrized for the 2 h period using a value of 3 mg m^{-3} at 10 min and a wall-loss rate of 10% h^{-1} determined from the filter mass and SMPS measurements. For gas-wall partitioning calculations the same SIMPOL.1-calculated vapor pressures were used, the equivalent absorbing wall mass concentration was taken to be 10 mg m^{-3}, and the time scale for reaching gas-wall partitioning equilibrium was taken to be 10 min. The predicted moles of each product collected on the filter during the 2 h sampling period was calculated by summing the model-predicted values for particles at each time interval. The molar yields of particle-phase products were calculated from these values, the volume of air sampled, and the 1 ppm of α-pinene reacted; and then used to calculate SOA molar yields of peroxide, carbonyl (aldehydes + ketones), carboxyl, hydroxyl, ester, and methylene groups, and the total SOA molar and mass yields. The calculated functional group composition was used in the same way as the measured values to calculate SOA O/C and H/C ratios, molecular weight, saturation concentration, and density.

RESULTS AND DISCUSSION

Mechanism of Formation of SOA from the Reaction of α-Pinene with O_3. To interpret the functional group composition of SOA formed in these experiments, it is necessary to first understand the major gas- and particle-phase reactions by which each of the quantified functional groups can be added to products. Although the full mechanism of the reaction of α-pinene with O_3 is not yet understood, most of the basic reaction pathways that can lead to the addition of specific groups are reasonably well-known.[2] In Figures 1 and 2 we show examples of gas- and particle-phase pathways that can lead to the addition of peroxide (hydroperoxide, dialkyl peroxide, peroxycarboxyl, secondary ozonide), carbonyl (aldehyde, ketone), hydroxyl, carboxyl, and ester groups. The functional group composition of the SOA also depends on gas-particle partitioning and therefore compound vapor pressure. According to the SIMPOL.1 group contribution method,[46] hydroperoxide, dialkyl peroxide, aldehyde, ketone, hydroxyl, carboxyl, and ester groups reduce compound vapor pressures by factors of about 300, 2, 20, 10, 200, 4000, and 20, respectively, although compound vapor pressures are also influenced by the arrangement of functional groups (i.e., isomer structure) and their interactions within the molecule.

Gas-Phase Reactions. The proposed initial steps in the reaction of α-pinene with O_3 (with estimated branching ratios) are shown in Figure 1.[9,25] The reaction is initiated by the addition of O_3 to the C═C double bond to form an unstable primary ozonide, which rapidly decomposes equally to form two excited Criegee intermediates (ECI 1 and 2) that contain both a carbonyl and carbonyl oxide group. The ECI can be collisionally stabilized to form stabilized Criegee intermediates (SCI 1 and 2), or they can undergo isomerization or decomposition reactions through the vinyl hydroperoxide (VHP) pathway to produce organoperoxy radicals ($RO_2^\bullet$ 1, 2, and 3) + OH radicals.[9] It is estimated that ~77% of ECI undergo isomerization or decomposition through the VHP pathway to yield $RO_2^\bullet$ radicals, while the rest are stabilized to SCI (~15%) or isomerize to pinonic acid (~8%).[9,25−27] In the High-VOC experiments, all the α-pinene reacted with O_3, whereas in the Low-VOC experiments ~80% reacted with O_3 and ~20% with OH radicals formed in the reaction. Thus, in the Low-VOC experiments, ~25% of the $RO_2^\bullet$ radicals would have somewhat different structures from those shown in Figure 1, although many of the subsequent reaction pathways should be similar. Furthermore, in the dry experiments the SCI react with carboxylic acids and aldehydes to form hydroperoxy esters and secondary ozonides, whereas under humid conditions they react with water vapor to form hydroxy hydroperoxides.

The reactions of $RO_2^\bullet$ radicals and resulting products depend on the VOC and NO_x concentration regimes. When NO_x concentrations are sufficiently low (as in these experiments), $RO_2^\bullet$ radicals react with HO_2 or $RO_2^\bullet$ radicals or they undergo intramolecular H-shift isomerization reactions. Reactions with HO_2 can form hydroperoxides, peroxycarboxylic acids, or carboxylic acids, whereas reactions with $RO_2^\bullet$ radicals can form dialkyl (or diacyl or mixed alkyl-acyl) peroxides, carbonyls, or alcohols.[2] Reactions with HO_2 or $RO_2^\bullet$ radicals can also form alkoxy radicals ($RO^\bullet$), which will either decompose to form carbonyls + alkyl (or acyl) radicals or isomerize and add O_2 to form hydroxyperoxy radicals, depending on the structure of the molecule.[55,56] Isomerization of $RO_2^\bullet$ radicals leads to the addition of hydroperoxide or peroxycarboxyl groups by chain propagation and carbonyl groups by chain termination, and are presumed to be the route by which HOMs are formed. These so-called autoxidation pathways propagate the radical species and rapidly add multiple functional groups to the molecule.[16,19,57]

Particle-Phase Reactions. The mechanisms of the major particle-phase reactions expected to contribute to SOA formation are shown in Figure 2. These include Baeyer−Villiger reactions in which peroxycarboxylic acids and hydroperoxides react with carbonyls to form acylperoxy hemiacetals and peroxy hemiacetals that decompose to carboxylic acids, esters, and alcohols; and reactions of alcohols and carbonyls to form hemiacetals and acetals.[2,58−60] When hydroperoxy esters and hydroxy hydroperoxides (formed from reactions of SCI with carboxylic acids or with water, respectively) undergo these particle-phase reactions, they are converted to hydroxy esters and gem-diols, with the latter decomposing to water and pinonaldehyde that should evaporate from the SOA either in the chamber or during filter sampling. On the basis of a number of studies that have employed mass spectrometry to show that oligomers contribute significantly to the SOA formed from α-pinene ozonolysis,[13,61,62] particle-phase reactions are expected to be important in the experiments conducted here.

Interpretation of Functional Group Composition of SOA. The SOA is composed of compounds with a range of carbon numbers, which is not determined in our analyses. For presentation purposes, the composition is therefore reported as the average number of each functional group per C_{10} molecule, the carbon number of α-pinene. Using this approach, our analysis of the functional group composition provided the following information about the SOA: (1) number of each functional group per C_{10} molecule, (2) total number of functional groups per C_{10} molecule, (3) total number of oxygen atoms per C_{10} molecule, and (4) O/C and H/C atomic ratios.

It is important to note here that the total number of functional groups in a molecule is determined predominantly by gas-phase reactions (Figure 1), with particle-phase reactions mostly serving to convert one type of functional group to another, usually through H atom and/or O atom transfer (Figure 2). This is always the case when reactions of peroxycarboxylic acids or hydroperoxides with carbonyls go

DOI: 10.1021/acsearthspacechem.8b00117
ACS Earth Space Chem. 2018, 2, 1196−1210

Table 1. Results of Measurements and MCM Modeling of the Functional Group Composition of SOA Formed from Reactions of α-Pinene with O_3 under a Variety of Conditions

	High-VOC			Low-VOC	
	measurement		MCM model	measurement	
	dry	humid	dry/humid	dry	humid
functional group	(functional group/C_{10} molecule[a])				
peroxide [HCOOH]	0.13 ± 0.04	0.11 ± 0.02	0.63/0.68	1.00 ± 0.01	0.44 ± 0.2
ester [O═COR]	0.82 ± 0.04	0.25 ± 0.06	0.20/0.00	0.88 ± 0.1	1.29 ± 0.1
carbonyl [C═O]	1.20 ± 0.04	1.15 ± 0.2	1.72/1.65	0.74 ± 0.1	0.99 ± 0.2
carboxyl [O═COH]	1.37 ± 0.1	1.28 ± 0.1	0.24/0.21	0.71 ± 0.03	1.48 ± 0.4
hydroxyl [HCOH]	0.24 ± 0.02	0.14 ± 0.1	0.50/0.75	0.13 ± 0.04	0.18 ± 0.1
total FG	3.76 ± 0.1	2.93 ± 0.3	3.29/3.29	3.46 ± 0.1	4.38 ± 0.5
methylene [CH_2]	6.24 ± 0.1	7.07 ± 0.3	6.71/6.71	6.54 ± 0.1	5.62 ± 0.5

[a]Uncertainties are standard deviations calculated from replicate experiments.

Table 2. Results of Measurements and MCM Modeling of Chemical Properties and Yields of SOA Formed from Reactions of α-Pinene with O_3 under a Variety of Conditions

	High-VOC			Low-VOC	
	measurement		MCM model	measurement	
	dry	humid	dry/humid	dry	humid
O/C	0.61 ± 0.05	0.46 ± 0.09	0.44/0.42	0.61 ± 0.06	0.76 ± 0.23
H/C	1.46 ± 0.13	1.59 ± 0.22	1.59/1.65	1.60 ± 0.08	1.40 ± 0.56
MW	232 ± 1	209 ± 3	206/203	233 ± 1	255 ± 14
C* (μg m^{-3})	1 ± 0.2	6 ± 2	70/45	2 ± 0.5	0.02 ± 0.01
density (g/mL)	1.38 ± 0.03	1.24 ± 0.05	1.23/1.20	1.33 ± 0.02	1.49 ± 0.13
SOA mass yield	0.78 ± 0.04	0.45 ± 0.05	1.0/0.93	0.22 ± 0.03	0.24 ± 0.03
SOA molar yield	0.45 ± 0.02	0.30 ± 0.03	0.68/0.62	0.13 ± 0.01	0.13 ± 0.02

[a]Uncertainties are standard deviations calculated from replicate experiments.

to completion (Baeyer−Villiger reactions), thereby forming the same number of products as reactants (Figure 2), but it does not necessarily hold when stable oligomers are formed that do not decompose to a pair of products. In the latter case, the outcome depends on the type of oligomer formed since they can affect the analysis of functional groups in different ways. We can summarize possible effects or noneffects of the oligomers shown in Figure 2 on functional group analyses[22,23] as follows: (1) ester and carboxyl groups are accurately quantified since they do not participate in the oligomer formation/dissociation equilibria; (2) peroxide groups are accurately quantified regardless of oligomer formation/dissociation equilibria; (3) secondary ozonides, hemiacetals, and acetals (other than those formed from cyclic hemiacetals) are hydrolyzed to the original monomers during carbonyl analysis, so the carbonyl groups in the monomers are quantified; (4) hydroxyl groups are accurately quantified in hemiacetals regardless of the formation/dissociation equilibrium but are not quantified if peroxy or acylperoxy hemiacetals dissociate to the original monomers; and (5) acylperoxy groups are accurately quantified in both carboxyl and peroxide analysis, but because of the short lifetime of acylperoxy hemiacetals,[60] they likely decompose irreversibly prior to analysis. Furthermore, although the measured functional group composition of SOA is affected by particle-phase reactions that occur in the chamber and during filter sampling, the types of reactions and products should be similar regardless of where they occur. This should be the case for reactions that might occur during filter extraction and functional group analysis as well, with the most likely changes being due to dissociation of oligomers to the original monomers upon dilution in solvents.

High-VOC Experiments. These experiments were conducted with a high concentration of α-pinene (1 ppm) and excess O_3 (2 ppm) in order to achieve a lifetime for α-pinene of ∼5 min, thus reducing the loss of products by gas-wall partitioning that would occur on a similar time scale in the absence of particles[30] but on a much longer time scale at the high SOA mass concentrations formed here.[31] Because of the shorter bimolecular reaction time scales achieved under these conditions, products formed through $RO_2^\bullet$ + $RO_2^\bullet$ or $RO_2^\bullet$ + HO_2 reactions should be enhanced relative to Low-VOC conditions, and the autoxidation reactions (which are not included in the MCM model) that lead to HOMs should be less important. Nonetheless, although the SOA composition simulated using the MCM model provides a useful starting point for interpreting the measurements, the comparison has a number of limitations: (1) the α-pinene + O_3 reaction mechanism is based on poorly constrained reaction rate constants and branching ratios; (2) estimated vapor pressures used to calculate gas-particle partitioning of multifunctional compounds can be in error by 1−2 orders of magnitude; and (3) the model does not include particle-phase reactions.

The results of measurements and MCM modeling of the functional group composition and other properties of SOA formed in the High-VOC experiments conducted in dry (∼0% RH) and humid (50% and 85% RH) air are listed in Table 1 and Table 2 and shown in bar graph form in Figure S1. Model results are reported for dry/humid conditions since results for 50% and 85% RH were essentially the same. Similarly, because measured values for all functional groups except esters showed

DOI: 10.1021/acsearthspacechem.8b00117
ACS Earth Space Chem. 2018, 2, 1196−1210

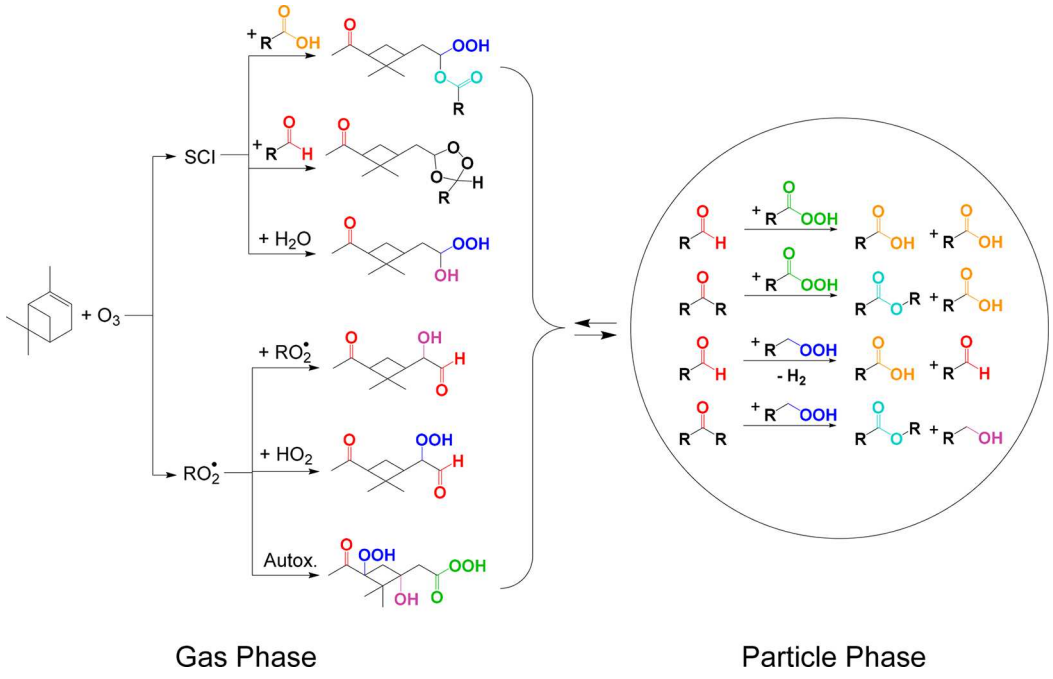

Figure 3. Simplified schematic showing the formation of functional groups through gas-phase chemistry, and their possible fate once they partition into the aerosol and are vulnerable to particle-phase reactions that alter their functionality.

no clear trend with humidity, in the following discussion average measured values are also presented for dry/humid conditions, where the humid values are the average for 50% and 85% RH. Results for all experiments are given in Table S1 and Table S2.

SOA Functional Group Composition. The number of functional groups per C_{10} molecule measured for dry/humid conditions were as follows: 0.13/0.11 peroxide, 0.82/0.25 ester, 1.20/1.15 carbonyl, 1.37/1.28 carboxyl, and 0.24/0.14 hydroxyl, for a total of 3.76/2.93 and thus 6.24/7.07 methylene groups, whereas the number obtained from the MCM model were in general quite different: 0.63/0.68 peroxide, 0.20/0.00 ester, 1.72/1.65 carbonyl, 0.24/0.21 carboxyl, and 0.50/0.75 hydroxyl, but with similar totals of 3.29/3.29 and thus 6.71/6.71 methylene groups. The measurements show that the SOA composition was dominated by carbonyl and carboxyl groups, with far fewer peroxide, ester, and hydroxyl groups; and that except for esters humidity had little effect on the functional group composition. The measured 3.76/2.93 functional groups are consistent with the 3.29/3.29 functional groups predicted by the MCM model for products of $RO_2^\bullet$ + $RO_2^\bullet$ and $RO_2^\bullet$ + HO_2 reactions (Figure 1), with the presence of more than three functional groups in a product indicating the occurrence of either alkoxy or $RO_2^\bullet$ radical isomerization via H atom abstraction (noting that abstraction of an aldehydic H atom does not add a functional group, but only converts it to something else).

As can be seen in Figure 1 and in the MCM model results for carbonyls (1.72/1.65), the products are generally predicted to contain 1−3 carbonyl groups per molecule, on average significantly more than the measured values of 1.20/1.15. This discrepancy can be explained by the occurrence of particle-phase reactions in which aldehyde and ketone groups are oxidized to carboxyl and ester groups, respectively, by Baeyer−Villiger reactions involving hydroperoxide or peroxycarboxyl groups (Figure 2) formed by $RO_2^\bullet$ + HO_2 or $RO_2^\bullet$ radical isomerization reactions. Such reactions also help to explain the presence of 1.37/1.28 carboxyl groups and 0.82/0.25 ester groups per C_{10} molecule. Although carboxyl groups can be formed in the gas-phase through the "hot-acid" decomposition channel to form pinonic acid, and through reactions of acylperoxy radicals with HO_2, the contribution of carboxyl groups to SOA predicted by the MCM model is only 0.24/0.21 per C_{10} molecule. Furthermore, the only known gas-phase mechanism for forming esters in these experiments is the reaction of SCI with carboxylic acids under dry conditions (which we added to the MCM model used here), although they can be formed by ozonolysis of dihydrofurans formed from cyclization and dehydration of hydroxycarbonyls in the presence of strong acid,[2] and Müller et al.[63] have suggested that the esters they identified by mass spectrometry in SOA formed by α-pinene ozonolysis might be formed by an unknown gas-phase radical mechanism. The MCM model thus under-predicts the number of ester groups measured per C_{10} molecule for both dry (0.20 compared to 0.82) and humid (0.00 compared to 0.25) conditions, although the predicted value of 0.20 due the reaction of SCI with carboxylic acids does account for some of the increase in measured ester groups from humid (0.25) to dry (0.82) conditions and could be more if the SCI yield is closer to 0.30[64] rather than the value of 0.15 used in the MCM model. We also note that esters could not have been formed via particle-phase decarboxylation of diacyl peroxides as proposed by Zhang et al.[65] since this requires an ionic aerosol matrix such as aqueous ammonium sulfate that was not present in our experiments. It thus appears that particle-phase oxidation of carbonyl groups contributes significantly to the formation of both carboxyl and ester groups in the SOA.

The peroxides that are formed in the gas phase and can subsequently oxidize carbonyl groups include peroxycarboxylic acids, hydroperoxides, hydroperoxy esters, and hydroxy hydroperoxides (Figures 1 and 2). The low peroxide content of the SOA of 0.13/0.11 peroxide groups per C_{10} molecule compared to the MCM model predictions of 0.63/0.68 is

DOI: 10.1021/acsearthspacechem.8b00117
ACS Earth Space Chem. 2018, 2, 1196−1210

consistent with significant loss of these compounds by particle-phase reactions, which can occur on time scales of a few hours or less.[21,60] The peroxides detected in the SOA may thus be residuals of these compounds or they may be relatively nonreactive dialkyl (or diacyl) peroxides formed with low yields (Figure 1) that are not included in the MCM model. These peroxides are known to be stable against thermal decomposition below ∼100 °C. They also were not exposed to strong acid that could catalyze decomposition,[51,66−68] although it is not known if carboxylic acids might instead serve as catalysts.[66]

The number of hydroxyl groups measured in SOA was also small, 0.24/0.14 per C_{10} molecule compared to 0.50/0.75 for the MCM model, indicating that the role of $RO_2^\bullet$ + $RO_2^\bullet$ or alkoxy radical isomerization reaction pathways by which they could have been formed (Figure 1) was less than that predicted by the MCM model. It is also possible, however, that particle-phase formation of acetals acted as a sink for hydroxyl groups (two hydroxyl groups are lost per one acetal formed in Figure 2) since acetals are not hydrolyzed back to alcohols under the basic conditions of the hydroxyl group analysis.[22]

The general gas- and particle-phase reactions that lead to formation and loss of the functional groups measured here are summarized in Figure 3. This scheme is relevant for both the High-VOC and Low-VOC reaction regimes, the latter of which will be discussed below.

Other SOA Properties and Yields. The O/C and H/C ratios, molecular weight, saturation concentration, and density calculated from the measured functional group composition for the dry/humid reactions were 0.61/0.46 and 1.46/1.59, 232/209 g mol^{-1}, 1/6 $\mu g\ m^{-3}$, and 1.38/1.24 g cm^{-3}, whereas the corresponding values obtained from the MCM model were 0.44/0.42 and 1.59/1.65, 206/203 g mol^{-1}, 70/45 $\mu g\ m^{-3}$, and 1.23/1.20 g cm^{-3}. The differences in the measured values for dry and humid reactions are in general a reflection of the larger number of functional groups in SOA formed in the dry (3.76) compared to humid (2.93) experiments, which led to higher O/C and lower H/C ratios, higher molecular weight and density, and lower saturation concentration. Differences in the MCM model predictions are small for the dry and humid experiments, due to the similar functional group compositions. For comparison, after correcting for AMS calibration[36] the O/C and H/C ratios extrapolated to high mass loadings reported by Kuwata et al.[47] for this reaction under dry conditions were 0.48 and 1.63, and their measured particle density was 1.25 g cm^{-3}.

The measured SOA mass and molar yields for the dry/humid reactions were 0.78/0.45 and 0.45/0.30, whereas those obtained from the MCM model were 1.0/0.93 and 0.68/0.62. The measured SOA molar yields mean that 45% and 30% of the α-pinene molecules that reacted formed SOA products under dry and humid conditions, with the rest either remaining in the gas phase or partitioning to the Teflon chamber walls.[30,31,42] The significantly higher SOA (mass/molar) yields measured for the dry (0.78/0.45) compared to humid (0.45/0.30) conditions is probably due to the differences in the fates of the hydroperoxy esters and hydroxy hydroperoxides formed from the reactions of SCI under dry and humid conditions, respectively. Although both of these products will partition to the particle phase and apparently undergo Baeyer−Villiger reactions as described above (Figure 2), the hydroxyesters formed under dry conditions from hydroperoxyesters are expected to be stable and have sufficiently low vapor pressure to remain in the SOA,[69] whereas the gem-diol formed under humid conditions from the hydroxy hydroperoxide is expected (in the presence of carboxylic acids)[70] to rapidly decompose to water and pinonaldehyde, which are sufficiently volatile to evaporate. For example, assuming an SCI yield of 0.15 (the value used in the MCM model), the SOA molar yield would be predicted to increase from 0.30 under humid conditions to at least 0.45 under dry conditions, depending on whether the hydroperoxy esters were formed by reaction of SCI with small or large carboxylic acids and thus more similar in size to C_{10} monomers or C_{20} dimers. The additional particulate mass from hydroxyesters should not only increase the SOA yield directly but also indirectly by enhancing the partitioning of semivolatile products due to the larger SOA mass concentration.

The measured and modeled SOA mass yields agree to within a factor of ∼2, which is quite good, considering that the model does not account for particle-phase reactions that are clearly important. In a previous comparison for this reaction Jenkin found that in order to achieve reasonable agreement between the measurements and MCM model predictions the estimated vapor pressures of all products had to be reduced by a factor of ∼120.[7] Although it was thought that this adjustment was needed to account for the effects of oligomer formation on product volatility, it may also have been due in part to inaccuracies in estimated vapor pressures that were orders of magnitude higher than those used here. For example, the subcooled liquid vapor pressures used by Jenkin[7] for pinonic acid, pinic acid, and 1-hydroxypinonic acid, three of the major low volatility products, were 4.3×10^{-3}, 4.7×10^{-4}, and 3.3×10^{-4} Torr, whereas the corresponding values used here (estimated using the SIMPOL.1 group contribution method of Pankow and Asher[46] rather than the empirical method used by Jenkin[7]) were 5.9×10^{-5}, 3.6×10^{-7}, and 3.4×10^{-7} Torr. Note, however, that group contribution methods such as SIMPOL.1 generally underestimate the vapor pressures of multifunctional compounds by not accounting for intermolecular effects like hydrogen bonding, and thus, the SIMPOL.1 method probably provides lower limits to compound vapor pressures.[71]

Low-VOC Experiments. These experiments were conducted with a low concentration of α-pinene (10 ppb) and excess O_3 (300 ppb) in order to increase time scales for $RO_2^\bullet$ + $RO_2^\bullet$ and $RO_2^\bullet$ + HO_2 reactions compared to High-VOC conditions, thus allowing enhanced $RO_2^\bullet$ radical isomerization and addition of hydroperoxide and peroxycarboxyl groups that are characteristic of autoxidation (Figure 1) and HOM formation.[15,57] These conditions also reduced the SOA mass loading, thus unfortunately enhancing the loss of products by gas-wall partitioning that occurs on a time scale of ∼18 min in this chamber.[30,31] The experiments were conducted under dry (∼0% RH) and humid (65% RH) conditions to probe the possible effects of water vapor on autoxidation reactions.

The results of measurements of the functional group composition and other properties of SOA formed in the Low-VOC experiments conducted in dry (∼0% RH) and humid (65% RH) air are listed in Table 1 and Table 2 and shown in Figure S1. Because the functional group composition showed a clear effect of humidity, in the following discussion measured average values are discussed for dry and humid conditions. Results for all experiments are given in Table S3 and Table S4. The proposed explanations for the results of these experiments are certainly speculative, given the current limited state of knowledge concerning the products of

DOI: 10.1021/acsearthspacechem.8b00117
ACS Earth Space Chem. 2018, 2, 1196−1210

autoxidation reactions for this system, which is limited to molecular formulas,[14−17] and the failure of theory to explain the observed rates of these reactions for α-pinene ozonolysis using plausible mechanisms.[20] Nonetheless, it is possible to show that the functional group composition of the SOA is roughly consistent with expectations when the $RO_2^•$ radicals formed are allowed to undergo autoxidation reactions comparable to those identified for simpler cycloalkenes,[19,72] and the subsequent products then react further in particles by Baeyer−Villiger reactions that appear to occur under High-VOC conditions.

Evidence for HOMs. In all dry and humid Low-VOC experiments gas-phase HOMs with elemental formulas identical to those measured under dry conditions by Ehn et al.[14,15] were detected using the NO_3−CIMS. As illustrated in Figure 4, the mass spectra for the dry and humid reactions are

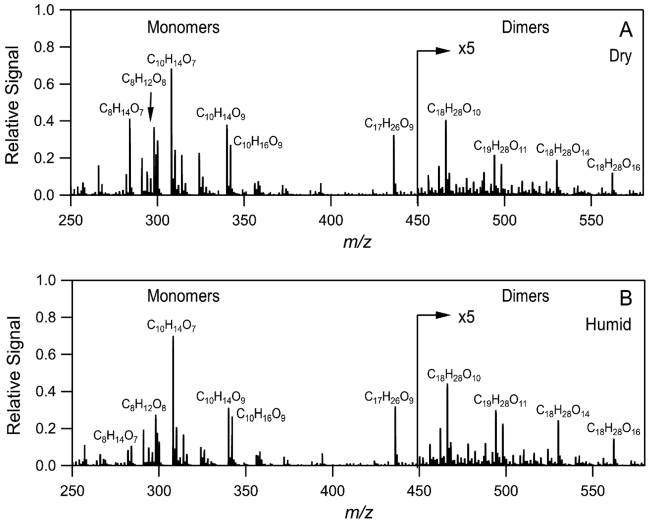

Figure 4. Mass spectra of gas-phase reaction products measured with the NO_3−CIMS during the (A) dry and (B) humid Low-VOC experiments. Compounds were detected as $C_xH_yO_z{\cdot}NO_3^-$ adducts.

similar and contain peaks that are indicative of HOM monomers and dimers previously identified by Ehn et al.[14,15] under dry conditions. For dry conditions, the O/C and H/C ratios calculated from the NO_3−CIMS spectra were 0.8 and 1.5, similar to the values of 0.7 and 1.5 reported by Ehn et al.,[14,15] and the O/C and H/C ratios of the SOA measured using a HR-ToF-AMS were 0.58 and 1.6, also in good agreement with the ratios of 0.7 and 1.5 reported by Ehn et al.[15] From this comparison, it appears that we were able to replicate the experimental conditions of earlier HOM studies and that the SOA analyzed here and results discussed below should also apply to SOA produced in that work.

SOA Functional Group Composition. The number of functional groups per C_{10} SOA molecule measured in the dry Low-VOC experiment were as follows: 1.00 peroxide, 0.88 ester, 0.74 carbonyl, 0.71 carboxyl, and 0.13 hydroxyl, for a total of 3.46, with 6.54 methylene groups. The measured number of functional groups in the dry Low-VOC SOA (3.46) was slightly lower than in the dry High-VOC SOA (3.76), but the amounts of specific functional groups differed significantly between these experiments. The larger number of peroxide groups in dry Low-VOC SOA (1.00) compared to dry High-VOC SOA (0.13) is indicative of a larger contribution from dialkyl and diacyl peroxides, which are relatively unreactive and thus able to persist in the SOA without undergoing decomposition reactions. This seems reasonable, given the much smaller mass of Low-VOC SOA (~5 μg m^{-3} compared to ~3000 μg m^{-3} for the High-VOC SOA), which leads to preferential partitioning by low volatility dimers rather than the monomers that appear to dominate the High-VOC SOA (at least prior to particle-phase oligomer formation). An example of diacyl peroxide formation followed by a Baeyer−Villiger reaction (shown here to be intramolecular for simplicity) is shown in Figure 5, where the $RO_2^•$ radical involved in the self-

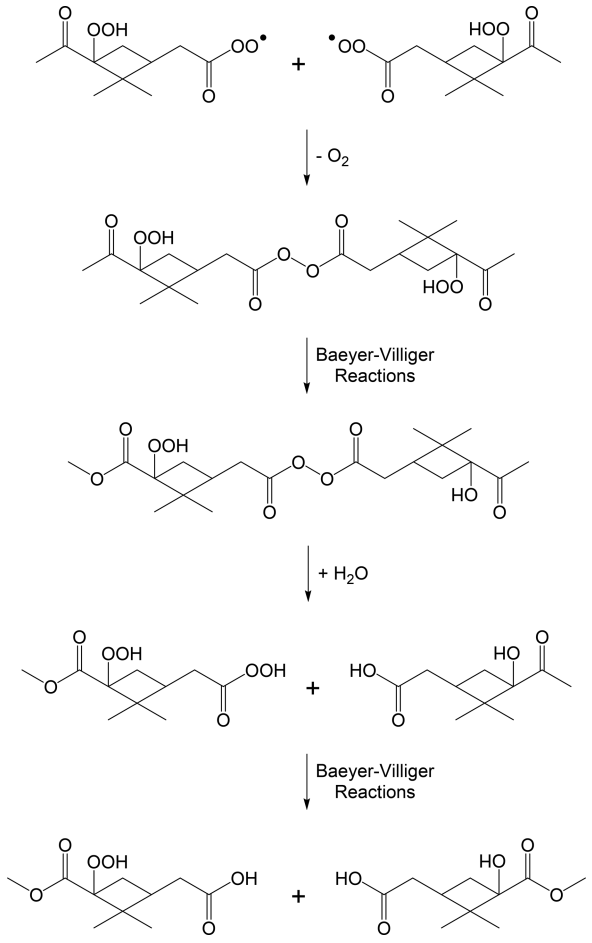

Figure 5. Schematic showing an example of the formation of a diacyl peroxide from the gas-phase self-reaction of $RO_2^•$ radicals, and subsequent particle-phase hydrolysis and Baeyer−Villiger reactions leading to the formation of peroxycarboxylic acid, carboxylic acid, and ester groups.

reaction is one that is proposed to lead to autoxidation products in Figure 1. For this compound the number of peroxide, ester, carbonyl, carboxyl, and hydroxyl groups per C_{10} molecule that would be reported from functional group analysis are 1.0, 0.5, 0.5, 1.0, and 0.5, for a total of 3.5 since the diacyl peroxide group would be measured as one peroxide and two carboxyl groups. These values agree reasonably well with the measured SOA composition (1.0, 0.71, 0.88, 0.74, and 0.13 for a total of 3.46). The lower-than-expected measured number of hydroxyl groups may be due to formation of acetals in the particles, which are not hydrolyzed back to monomers in the analysis.

The number of functional groups per C_{10} SOA molecule measured in the humid Low-VOC experiment were as follows:

DOI: 10.1021/acsearthspacechem.8b00117
ACS Earth Space Chem. 2018, 2, 1196−1210

0.44 peroxide, 1.29 ester, 0.99 carbonyl, 1.48 carboxyl, and 0.18 hydroxyl, for a total of 4.38, with 5.62 methylene groups. The 4.38 functional groups are significantly higher than the 3.46 measured in the dry Low-VOC SOA, with the number of peroxide groups decreasing from 1.00 to 0.44; the number of ester, carbonyl, and carboxyl groups increasing from 0.88, 0.74, and 0.71 to 1.29, 0.99, and 1.48; and the number of hydroxyl groups remaining about the same at 0.13 and 0.18. These differences are not due to an influence of water on the functional group analysis since any water is removed during the SOA extraction and drying process. The simplest explanation for the increased number of functional groups measured under humid conditions is that water somehow enhanced the fraction of $RO_2^\bullet$ radicals that isomerized, which would increase the number of functional groups per C_{10} molecule and the O/C ratio. This could occur if water either increased the rate of isomerization or reduced the rate of chain termination. However, quantum chemical calculations predict, for example, that at 50% RH and 298 K only ~1% of $CH_2(OH)CH_2O_2^\bullet$ and $CH_3C(O)CH_2O_2^\bullet$ radicals are complexed with water,[73] so the extent to which water might impact $RO_2^\bullet$ radical isomerization or termination reactions seems limited. It may be that these effects are enhanced for larger multifunctional compounds, but the similarity in the NO_3−CIMS mass spectra obtained under dry and humid conditions (Figure 4) does not support this. Additional studies are needed to understand the effect of humidity on autoxidation reactions.

An alternative explanation for the effect of humidity on functional group composition is that particulate diacyl peroxides are hydrolyzed by water taken up by the particles, even though the amount absorbed is expected to be small at 65% RH.[74] Kinetics studies[75] have shown that diacyl peroxides can be hydrolyzed to a peroxycarboxylic acid and carboxylic acid in water (although sulfuric acid was used as a catalyst in the reactions studied), which as shown in Figure 5 would affect the functional group composition by eliminating one peroxide group and forming one ester group via a Baeyer−Villiger reaction. For these products the number of peroxide, ester, carbonyl, carboxyl, and hydroxyl groups per C_{10} molecule that would be reported from functional group analysis are 0.50, 1.0, 0.0, 1.0, and 0.5, for a total of 3.0. With the exception of the carbonyl groups, this composition compares reasonably well with the measured SOA composition (0.44, 1.48, 1.29, 0.99, and 0.18 for a total of 4.38). It may be that small carbonyl compounds such as formaldehyde were taken up by the SOA during filter sampling, forming peroxyhemiacetals that can then dissociate back to the hydroperoxide and aldehyde during analysis. We have previously observed this reaction when SOA containing hydroperoxides (formed from the ozonolysis of 1-tetradecene in the presence of an alcohol) were exposed to formaldehyde.[68] It would also be consistent with measurements made by Mutzel et al.,[17] who detected large amounts of particle-phase C_1−C_4 carbonyl compounds, including formaldehyde, acetaldehyde, acetone, and methyl glyoxal, while studying HOM formation under conditions similar to the Low-VOC experiments conducted here. Such uptake would also increase the number of functional groups per C_{10} molecule, possibly explaining the increase observed for humid conditions.

Other SOA Properties and Yields. The average O/C and H/C ratios calculated for the dry Low-VOC experiments from the functional group composition were 0.61 and 1.60, the average molecular weight and density were 233 g mol^{-1} and 1.33 g cm^{-3}, and the average SOA mass and molar yields were 0.22 and 0.13, whereas the corresponding values calculated for the humid experiments were 0.76 and 1.40, 255 g mol^{-1} and 1.49 g cm^{-3}, and 0.24 and 0.13. The differences in O/C and H/C ratios and molecular weight and density are in general a reflection of the larger number of functional groups in SOA formed in the humid compared to dry experiments, but this appears to have had no significant effect on SOA yields. Also, for comparison, the O/C and H/C ratios of the SOA measured using a HR-ToF-AMS were 0.58 and 1.6 in one dry experiment, and the average values measured in two humid experiments were 0.54 and 1.69 (Table S4). The values measured with the HR-ToF-AMS and from functional group analysis agree very well for the dry experiment (0.58 and 1.60 compared to 0.61 and 1.60) but less well for the humid experiments (0.54 and 1.69 compared to 0.67 and 1.45). One possible explanation for the discrepancy in the humid experiments is that the previously proposed uptake of small carbonyl-containing compounds during filter sampling altered the SOA composition from what it was in the chamber when the HR-ToF-AMS measurements were made.

■ CONCLUSIONS

It is shown here that functional group analysis of SOA formed from the ozonolysis of α-pinene over a range of α-pinene concentrations and relative humidities can provide information on the products and mechanisms of the gas- and particle-phase reactions involved in SOA formation. These methods, which employ derivatization and spectrophotometry to quantify the contributions of peroxide, carbonyl, carboxyl, hydroxyl, and ester groups, are especially useful for providing top-down constraints on studies of SOA formation from VOC oxidation reactions such as this one, where reaction mechanisms are still not well understood and the SOA composition is extremely complex (in this case containing many hundreds of compounds). When the functional group composition is normalized to the carbon number of the parent VOC (in this case C_{10}), the results can be used to estimate the number of each functional group per C_{10} molecule, the total number of functional groups per C_{10} molecule, the total number of oxygen atoms per C_{10} molecule, and the O/C and H/C ratios. In general, the total number of functional groups in a molecule is determined predominantly by gas-phase reactions, with subsequent particle-phase reactions converting one type of functional group to another (usually through H atom and/or O atom transfer) and, in some cases, reducing the number of functional groups via oligomer formation. This information can be useful for developing and evaluating models of VOC oxidation and SOA formation, for which comparisons are usually limited to SOA yields and O/C ratios and perhaps a few molecular products. Here, we compared the results of experiments conducted with high VOC concentrations to simulations conducted using the Master Chemical Mechanism with gas-particle and gas-wall partitioning theories since most of the products formed SOA, and thus, artifacts due to gas-wall partitioning were minimized. It would also be interesting to explore the possibility of developing compilations of SOA functional group yields for major VOC-oxidant systems, similar to those available for SOA yields, which might then be used in parametrized form in atmospheric models.

In the high VOC concentration experiments the gas-phase products that contributed to SOA formation appeared to be similar under dry and humid conditions and consist primarily of monomers containing on average a total of 3−4 peroxide,

DOI: 10.1021/acsearthspacechem.8b00117
ACS Earth Space Chem. 2018, 2, 1196−1210

carbonyl, carboxyl, or hydroxyl groups per C_{10} molecule formed through $RO_2^\bullet + RO_2^\bullet$ and $RO_2^\bullet + HO_2$ reactions, with a minor contribution from ester group-containing dimers that were formed under dry conditions from reactions of stabilized Criegee intermediates with carboxylic acids. Although the total number of functional groups per C_{10} molecule determined from SOA measurements was similar to that predicted by the MCM model, the distribution of functional groups differed considerably. In particular, measured amounts of carboxyl and ester groups were significantly larger than those predicted by the model, whereas peroxide, carbonyl, and hydroxyl groups were significantly smaller. A plausible explanation for this discrepancy is that aldehyde and ketone groups were converted to carboxyl and ester groups, respectively, through particle-phase Baeyer−Villiger reactions with hydroperoxides and peroxycarboxylic acids, thus adding carboxyl and ester groups while removing peroxide groups. The small measured amounts of hydroxyl groups indicate that alkoxy radical isomerization was less important than predicted by the model and may also have been due to particle-phase formation of acetals, which converts these groups (but not the carbonyl groups in the reaction partners) to a form that is not detected in the functional group analysis. It is also noteworthy that, despite the similar functional group composition measured in the dry and humid experiments, the SOA yield was significantly larger under dry conditions. This may have been due to formation of low-volatility ester group-containing dimers from reactions of stabilized Criegee intermediates with carboxylic acids under dry conditions and subsequent enhanced partitioning of other semivolatile products due to the larger SOA mass concentration. Furthermore, although the measured and simulated functional group composition of the SOA differed significantly, the SOA yields agreed to within a factor of ∼2. This was probably due in large part to the similar total number of measured and simulated functional groups and the high SOA mass concentrations formed under these conditions, which resulted in gas-to-particle partitioning of a large fraction of the products and thus reduced the sensitivity of the SOA yield prediction to errors in gas-phase composition and the absence of particle-phase chemistry.

In the low VOC concentration experiments, conditions were achieved that resulted in the formation of gas-phase HOMs, apparently due to increased time scales for $RO_2^\bullet + RO_2^\bullet$ and $RO_2^\bullet + HO_2$ reactions that enhanced competition with $RO_2^\bullet$ radical isomerization and the formation of ROOR dimers from $RO_2^\bullet$ self-reactions. Because of the absence of $RO_2^\bullet$ radical isomerization pathways in the MCM and much greater expected loss of products by gas-wall partitioning, no attempt was made to model these experiments. The total number of functional groups per C_{10} molecule measured in these experiments ranged from about 3−5 and was higher for humid than dry conditions. In addition, the distribution of functional groups varied significantly: more peroxide groups for dry conditions; more carbonyl, carboxyl, and ester groups for humid conditions; and similar low amounts of hydroxyl groups for both conditions. Although explanations for these results are more speculative than for the high VOC concentration experiments, the functional group composition of the SOA can be plausibly explained based on the same gas- and particle-phase reactions that appear to occur under those conditions, but with the addition of autoxidation reactions, gas-phase dimer formation, particle-phase hydrolysis reactions, and gas-to-particle partitioning of small carbonyl compounds. In particular, it appears that the larger number of peroxide groups is due to enhanced $RO_2^\bullet$ isomerization and contributions from dimers containing dialkyl and diacyl peroxide groups, which are unreactive under dry conditions. Under humid conditions, however, diacyl peroxide groups are apparently hydrolyzed to carboxyl and peroxycarboxyl groups, with the latter then undergoing Baeyer−Villiger reactions that convert aldehyde and ketone groups to carboxyl and ester groups. Although this proposed mechanism should lead to fewer carbonyl groups under humid conditions, the slight increase that is observed may be due to enhanced gas-to-particle partitioning of small carbonyl compounds that subsequently react with hydroperoxides to form peroxyhemiacetals.

■ ASSOCIATED CONTENT

Supporting Information

The Supporting Information is available free of charge on the ACS Publications website at DOI: 10.1021/acsearthspacechem.8b00117.

Bar graph of measured and modeled functional group compositions. Reported functional group compositions, SOA properties, and yields from individual experiments conducted for the High-VOC and Low-VOC systems (PDF)

■ AUTHOR INFORMATION

Corresponding Author

*E-mail: Paul.Ziemann@colorado.edu.

ORCID

Megan S. Claflin: 0000-0003-0878-8712
Jose L. Jimenez: 0000-0001-6203-1847
Paul J. Ziemann: 0000-0001-7419-0044

Present Addresses

§Aerodyne Research, Inc., Billerica, Massachusetts 01821, United States.
‖State Key Laboratory of Organic Geochemistry and Guangdong Key Laboratory of Environment Protection and Resources Utilization, Guangzhou Institute of Geochemistry, Chinese Academy of Sciences, Guangzhou 510640, China.

Notes

The authors declare no competing financial interest.

■ ACKNOWLEDGMENTS

This material is based on work supported by the U.S. Environmental Protection Agency (EPA) under Grant RD-83540801 and an EPA STAR Fellowship FP-91770901-0 for Jordan Krechmer, by the National Science Foundation (NSF) under Grant AGS-1420007, and by DOE (BER/ASR) DE-SC0016559. This work has not been formally reviewed by the EPA, and the views expressed in this document are solely those of the authors, and the EPA does not endorse any products or commercial services mentioned in this publication.

■ REFERENCES

(1) Guenther, A.; Jiang, X.; Heald, C. L.; Sakulyanontvittaya, T.; Duhl, T.; Emmons, L. K.; Wang, X. The Model of Emissions of Gases and Aerosols from Nature version 2.1 (MEGAN2.1): An Extended and Updated Framework for Modeling Biogenic Emissions. *Geosci. Model Dev.* **2012**, *5*, 1471−1492.

(2) Ziemann, P. J.; Atkinson, R. Kinetics, Products, and Mechanisms of Secondary Organic Aerosol Formation. *Chem. Soc. Rev.* **2012**, *41*, 6582.

DOI: 10.1021/acsearthspacechem.8b00117
ACS Earth Space Chem. 2018, 2, 1196−1210

(3) Zhang, Q.; Jimenez, J. L.; Canagaratna, M. R.; Allan, J. D.; Coe, H.; Ulbrich, I.; Alfarra, M. R.; Takami, A.; Middlebrook, A. M.; Sun, Y. L. Ubiquity and Dominance of Oxygenated Species in Organic Aerosols in Anthropogenically-Influenced Northern Hemisphere Midlatitudes. *Geophys. Res. Lett.* **2007**, *34*, L13801.
(4) Pöschl, U. Atmospheric Aerosols: Composition, TransFormation, Climate and Health Effects. *Angew. Chem., Int. Ed.* **2005**, *44*, 7520−7540.
(5) Hallquist, M.; Wenger, J. C.; Baltensperger, U.; Rudich, Y.; Simpson, D.; Claeys, M.; Dommen, J.; Donahue, N. M.; George, C.; Goldstein, A. H.; et al. The Formation, Properties and Impact of Secondary Organic Aerosol: Current and Emerging Issues. *Atmos. Chem. Phys.* **2009**, *9*, 5155−5236.
(6) Yu, J.; Cocker, D. R.; Griffin, R. J.; Flagan, R. C.; Seinfeld, J. H. Gas-Phase Ozone Oxidation of Monoterpenes: Gaseous and Particulate Products. *J. Atmos. Chem.* **1999**, *34*, 207−258.
(7) Jenkin, M. E. Modelling the Formation and Composition of Secondary Organic Aerosol from α- and β-Pinene Ozonolysis Using MCM v3. *Atmos. Chem. Phys.* **2004**, *4*, 1741−1757.
(8) Lee, A.; Goldstein, A. H.; Keywood, M. D.; Gao, S.; Varutbangkul, V.; Bahreini, R.; Ng, N. L.; Flagan, R. C.; Seinfeld, J. S. Gas-Phase Products and Secondary Aerosol Yields from the Ozonolysis of Ten Different Terpenes. *J. Geophys. Res.* **2006**, *111*, D07302.
(9) Capouet, M.; Müller, J. F.; Ceulemans, K.; Compernolle, S.; Vereecken, L.; Peeters, J. Modeling Aerosol Formation in Alpha-Pinene Photo-oxidation Experiments. *J. Geophys. Res.* **2008**, *113*, D02308.
(10) Kowalewski, K.; Gierczak, T. Multistep Derivatization Method for the Determination of Multifunctional Oxidation Products from the Reaction of α-Pinene with Ozone. *J. Chromatogr.* **2011**, *1218*, 7264−7274.
(11) Atkinson, R.; Arey, J. Atmospheric Degradation of Volatile Organic Compounds. *Chem. Rev.* **2003**, *103*, 4605−4638.
(12) Griffin, R. J.; Cocker, D. R.; Flagan, R. C.; Seinfeld, J. H. Organic Aerosol Formation from the Oxidation of Biogenic Hydrocarbons. *J. Geophys. Res.* **1999**, *104*, 3555−3567.
(13) Docherty, K. S.; Wu, W.; Lim, Y. B.; Ziemann, P. J. Contributions of Organic Peroxides to Secondary Organic Aerosol formed from Reactions of Monoterpenes with O_3. *Environ. Sci. Technol.* **2005**, *39*, 4049−4059.
(14) Ehn, M.; Kleist, E.; Junninen, H.; Petäjä, T.; Lönn, G.; Schobesberger, S.; Dal Maso, M.; Trimborn, A.; Kulmala, M.; Worsnop, D. R.; et al. Gas Phase Formation of Extremely Oxidized Pinene Reaction Products in Chamber and Ambient Air. *Atmos. Chem. Phys.* **2012**, *12*, 5113−5127.
(15) Ehn, M.; Thornton, J. A.; Kleist, E.; Sipilä, M.; Junninen, H.; Pullinen, I.; Springer, M.; Rubach, F.; Tillmann, R.; Lee, B.; et al. A Large Source of Low-Volatility Secondary Organic Aerosol. *Nature* **2014**, *506*, 476−479.
(16) Mentel, T. F.; Springer, M.; Ehn, M.; Kleist, E.; Pullinen, I.; Kurten, T.; Rissanen, M.; Wahner, A.; Wildt, J. Formation of Highly Oxidized Multifunctional Compounds: Autoxidation of Peroxy Radicals Formed in the Ozonolysis of Alkenes − Deduced from Structure-Property Relationships. *Atmos. Chem. Phys.* **2015**, *15*, 6745−6765.
(17) Mutzel, A.; Poulain, L.; Berndt, T.; Iinuma, Y.; Rodigast, M.; Boge, O.; Richters, S.; Spindler, G.; Sipila, M.; Jokinen, T.; et al. Highly Oxidized Multifunctional Organic Compounds Observed in Tropospheric Particles: A Field and Laboratory Study. *Environ. Sci. Technol.* **2015**, *49*, 7754−7761.
(18) Mohr, C.; Lopez-Hilkiker, F. D.; Yli-Juuti, T.; Heitto, A.; Lutz, A.; Hallquist, M.; D'Ambro, E. L.; Rissanen, M. P.; Hao, L.; Schobesberger, S.; et al. Ambient Observations of Dimers from Terpene Oxidation in the Gas Phase: Implications for New Particle Formation and Growth. *Geophys. Res. Lett.* **2017**, *44*, 2958−2966.
(19) Rissanen, M. P.; Kurtén, T.; Sipiläj, M.; Thornton, J. A.; Kausiala, O.; Garmash, O.; Kjaergaard, H. G.; Petäjä, T.; Worsnop, D. R.; Ehn, M.; Kulmala, M. Effects of Chemical Complexity on the Autoxidation Mechanisms of Endocyclic Alkene Ozonolysis Products: From Methylcyclohexenes Toward Understanding α−Pinene. *J. Phys. Chem. A* **2015**, *119*, 4633−4650.
(20) Kurtén, T.; Rissanen, M. P.; Mackeprang, K.; Thornton, J. A.; Hyttinen, N.; Jørgensen, S.; Ehn, M.; Kjaergaard, H. G. Computational Study of Hydrogen Shifts and Ring-Opening Mechanisms in α-Pinene Ozonolysis Products. *J. Phys. Chem. A* **2015**, *119*, 11366−11375.
(21) Krapf, M.; Haddad, I. E.; Bruns, E. A.; Molteni, U.; Daellenbach, K. R.; Prevot, A. S. H.; Baltensperger, U.; Dommen, J. Labile Peroxides in Secondary Organic Aerosol. *Chem.* **2016**, *1*, 603−616.
(22) Aimanant, S.; Ziemann, P. J. Development of Spectrophotometric Methods for the Analysis of Functional Groups in Oxidized Organic Aerosol. *Aerosol Sci. Technol.* **2013**, *47*, 581−591.
(23) Ranney, A. P.; Ziemann, P. J. Microscale Spectrophotometric Methods for Quantification of Functional Groups in Oxidized Organic Aerosol. *Aerosol Sci. Technol.* **2016**, *50*, 881−892.
(24) Alvarado, A.; Arey, J.; Atkinson, R. Kinetics of the Gas-Phase Reactions of OH and NO_3 Radicals and O_3 with the Monoterpene Reactions Products Pinonaldehyde, Caronaldehyde, and Sabinaketone. *J. Atmos. Chem.* **1998**, *31*, 281−297.
(25) Atkinson, R. Gas-Phase Tropospheric Chemistry of Volatile Organic Compounds: 1. Alkanes and Alkenes. *J. Phys. Chem. Ref. Data* **1997**, *26*, 215−290.
(26) Rickard, A. R.; Johnson, D.; McGill, C. D.; Marston, G. OH Yields in the Gas-Phase Reactions of Ozone with Alkenes. *J. Phys. Chem. A* **1999**, *103*, 7656−7664.
(27) Paulson, S. E.; Chung, M. Y.; Hasson, A. S. OH Radical Formation from the Gas-Phase Reaction of Ozone with Terminal Alkenes and the Relationship Between Structure and Mechanism. *J. Phys. Chem. A* **1999**, *103* (41), 8125−8138.
(28) Eisele, F.; Tanner, D. Measurement of the Gas Phase Concentration of H_2SO_4 and Methane Sulfonic Acid and Estimates of H_2SO_4 Production and Loss in the Atmosphere. *J. Geophys. Res.* **1993**, *98*, 9001−9010.
(29) Jokinen, T.; Sipilä, M.; Junninen, H.; Ehn, M.; Lönn, G.; Hakala, J.; Petäjä, T.; Mauldin, R. L.; Kulmala, M.; Worsnop, D. R. Atmospheric Sulphuric Acid and Neutral Cluster Measurements using CI-APi-TOF. *Atmos. Chem. Phys.* **2012**, *12*, 4117−4125.
(30) Krechmer, J. E.; Pagonis, D.; Ziemann, P. J.; Jimenez, J. L. Quantification of Gas-Wall Partitioning in Teflon Environmental Chambers using Rapid Bursts of Low−Volatility Oxidized Species Generated In Situ. *Environ. Sci. Technol.* **2016**, *50*, 5757−5765.
(31) Krechmer, J. E.; Day, D. A.; Ziemann, P. J.; Jimenez, J. L. Direct Measurements of Gas/Particle Partitioning and Mass Accommodation Coefficients in Environmental Chambers. *Environ. Sci. Technol.* **2017**, *51*, 11867−11875.
(32) DeCarlo, P. F.; Kimmel, J. R.; Trimborn, A.; Northway, M. J.; Jayne, J. T.; Aiken, A. C.; Gonin, M.; Fuhrer, K.; Horvath, T.; Docherty, K. S.; et al. Field-Deployable, High-Resolution, Time-of-Flight Aerosol Mass Spectrometer. *Anal. Chem.* **2006**, *78*, 8281−8289.
(33) Hu, W. W.; Campuzano-Jost, P.; Day, D. A.; Croteau, P. L.; Canagaratna, M. R.; Jayne, J. T.; Worsnop, D. R.; Jimenez, J. L. Evaluation of the New Capture Vaporizer for Aerosol Mass Spectrometers (AMS) through Laboratory Studies of Inorganic Species. *Atmos. Meas. Technol. Discuss.* **2016**, 1−55.
(34) Xu, W.; Croteau, P.; Williams, L.; Canagaratna, M.; Onasch, T.; Cross, E.; Zhang, X.; Robinson, W.; Worsnop, D.; Jayne, J. Laboratory Characterization of an Aerosol Chemical Speciation Monitor with PM2.5 Measurement Capability. *Aerosol Sci. Technol.* **2017**, *51*, 1−15.
(35) Aiken, A. C.; Decarlo, P. F.; Kroll, J. H.; Worsnop, D. R.; Huffman, J. A.; Docherty, K. S.; Ulbrich, I. M.; Mohr, C.; Kimmel, J. R.; Sueper, D.; et al. O/C and OM/OC Ratios of Primary, Secondary, and Ambient Organic Aerosols with High-Resolution Time-of-Flight Aerosol Mass Spectrometry. *Environ. Sci. Technol.* **2008**, *42*, 4478−4485.
(36) Canagaratna, M. R.; Jimenez, J. L.; Kroll, J. H.; Chen, Q.; Kessler, S. H.; Massoli, P.; Hildebrandt Ruiz, L.; Fortner, E.; Williams,

DOI: 10.1021/acsearthspacechem.8b00117
ACS Earth Space Chem. 2018, 2, 1196−1210

L. R.; Wilson, K. R.; et al. Elemental Ratio Measurements of Organic Compounds Using Aerosol Mass Spectrometry: Characterization, Improved Calibration, and Implications. *Atmos. Chem. Phys.* **2015**, *15*, 253−272.
(37) Carlton, A. M.; de Gouw, J.; Jimenez, J. L.; Ambrose, J. L.; Brown, S.; Baker, K. R.; Brock, C. A.; Cohen, R. C.; Edgerton, S.; Farkas, C.; et al. The Southeast Atmosphere Studies (SAS): Coordinated Investigation and Discovery to Answer Critical Questions about Fundamental Atmospheric Processes. *Bull. Am. Meteorol. Soc.* **2018**, *99*, 547−567.
(38) Hu, W. W.; Campuzano-Jost, P.; Palm, B. B.; Day, D. A.; Ortega, A. M.; Hayes, P. L.; Krechmer, J. E.; Chen, Q.; Kuwata, M.; Liu, Y. J.; et al. Characterization of a Real-Time Tracer for Isoprene Epoxydiols-Derived Secondary Organic Aerosol (IEPOX−SOA) from Aerosol Mass Spectrometer Measurements. *Atmos. Chem. Phys.* **2015**, *15*, 11807−11833.
(39) Liu, J.; Russell, L. M.; Lee, A. K. Y.; McKinney, K. A.; Surratt, J. D.; Ziemann, P. J. Observations Evidence for Pollution-Influenced Selective Uptake Contributing to Biogenic Secondary Organic Aerosols in the Southeast U.S. *Geophys. Res. Lett.* **2017**, *44*, 8056−8064.
(40) Liu, J.; Russell, L. M.; Ruggeri, G.; Takahama, S.; Claflin, M. S.; Ziemann, P. J.; Pye, H. O. T.; Murphy, B. N.; Xu, L.; Ng, N. L.; McKinney, K. A.; Budisulistiorini, S. H.; Bertram, T. H.; Athanasios, N.; Surratt, J. D. Regional Similarities and NOx-Related Increases in Biogenic Secondary Organic Aerosol in Summertime Southeastern U.S. *J. Geophys. Res.* **2018**, DOI: 10.1029/2018JD028491.
(41) Yeh, G. K.; Claflin, M. S.; Ziemann, P. J. Products and Mechanism of the Reaction of 1−Pentadecane with NO_3 Radicals and the Effect of a − ONO_2 Group on Alkoxy Radical Decomposition. *J. Phys. Chem. A* **2015**, *119*, 10684−10696.
(42) Matsunaga, A.; Ziemann, P. J. Gas−Wall Partitioning of Organic Compounds in a Teflon Film Chamber and Potential Effects on Reaction Product and Aerosol Yield Measurements. *Aerosol Sci. Technol.* **2010**, *44*, 881−892.
(43) Zhang, X.; Cappa, C. D.; Jathar, S. H.; McVay, R. C.; Ensberg, J. J.; Kleeman, M. J.; Seinfeld, J. H. Influence of Vapor Wall Loss in Laboratory Chambers on Yields of Secondary Organic Aerosol. *Proc. Natl. Acad. Sci. U. S. A.* **2014**, *111*, 5802−5807.
(44) Nah, T.; McVay, R. C.; Zhang, X.; Boyd, C. M.; Seinfeld, J. H.; Ng, N. L. Influence of Seed Aerosol Surface Area and Oxidation Rate on Vapor Wall Deposition and SOA Mass Yields: A Case Study with α-Pinene Ozonolysis. *Atmos. Chem. Phys.* **2016**, *16*, 9361−9379.
(45) Banerjee, D. K.; Budke, C. C. Spectrophotometric Determination of Traces of Peroxides in Organic Solvents. *Anal. Chem.* **1964**, *36* (4), 792−796.
(46) Pankow, J. F.; Asher, W. E. SIMPOL.1: A Simple Group Contribution Methods for Predicting Vapor Pressures and Enthalpies of Vaporization of Multifunctional Organic Compounds. *Atmos. Chem. Phys.* **2008**, *8*, 2773−2796.
(47) Kuwata, M.; Zorn, S. R.; Martin, S. T. Using Elemental Ratios to Predict the Density of Organic Material Composed of Carbon, Hydrogen, and Oxygen. *Environ. Sci. Technol.* **2012**, *46*, 787−794.
(48) Jenkin, M. E.; Saunders, S. M.; Pilling, M. J. The Tropospheric Degradation of Volatile Organic Compounds: A Protocol for Mechanism Development. *Atmos. Environ.* **1997**, *31* (1), 81−104.
(49) Saunders, S. M.; Jenkin, M. E.; Derwent, R. G.; Pilling, M. J. Protocol for the Development of the Master Chemical Mechanism, MCM v3 (Part A): Tropospheric Degradation of Non−Aromatic Volatile Organic Compounds. *Atmos. Chem. Phys.* **2003**, *3* (1), 161−180.
(50) Tobias, H. J.; Ziemann, P. J. Kinetics of the Gas-Phase Reactions of Alcohols, Aldehydes, Carboxylic Acids, and Water with the C13 Stabilized Criegee Intermediate formed from Ozonolysis of 1−Tetradecene. *J. Phys. Chem. A* **2001**, *105*, 6129−6135.
(51) Tobias, H. J.; Docherty, K. S.; Beving, D. E.; Ziemann, P. J. Effect of Relative Humidity on the Chemical Composition of Secondary Organic Aerosol Formed from Reactions of 1-Tetradecene and O_3. *Environ. Sci. Technol.* **2000**, *34*, 2116−2125.
(52) Kanno, N.; Tonokura, K.; Tezaki, A.; Koshi, M. Water Dependence of the HO_2 Self Reaction: Kinetics of the HO_2-H_2O Complex. *J. Phys. Chem. A* **2005**, *109*, 3153−3158.
(53) Colville, C. J.; Griffin, R. J. The Roles of Individual Oxidants in Secondary Organic Aerosol Formation from Δ^3−carene: 2. SOA Formation and Oxidant Contribution. *Atmos. Environ.* **2004**, *38*, 4013−4023.
(54) Pankow, J. F. An Absorption Model of Gas/Particle Partitioning Involved in the Formation of Secondary Organic Aerosol. *Atmos. Environ.* **1994**, *28*, 189−193.
(55) Vereecken, L.; Peeters, J. Decomposition of Substituted Alkoxy Radicals−Part I: A Generalized Structure-Activity Relationship for Reaction Barrier Heights. *Phys. Chem. Chem. Phys.* **2009**, *11*, 9062−9074.
(56) Vereecken, L.; Peeters, J. A Structure−Activity Relationship for the Rate Coefficient of H−Migration in Substituted Alkoxy Radicals. *Phys. Chem. Chem. Phys.* **2010**, *12*, 12608−12620.
(57) Crounse, J. D.; Nielsen, L. B.; Jorgensen, S.; Kjaergaard, H. G.; Wennberg, P. O. Autoxidation of Organic Compounds in the Atmosphere. *J. Phys. Chem. Lett.* **2013**, *4*, 3513−3520.
(58) Patai, S. *The Chemistry of Peroxides*; John Wiley & Sons, 1983; Vol. 3.
(59) Wurster, C. F.; Durham, L. J.; Mosher, H. S. Peroxides. VII. The Thermal Decomposition of Primary Hydroperoxides. *J. Am. Chem. Soc.* **1958**, *80*, 327−331.
(60) Lubarsky, G. D.; Kagan, M. J. The Intermediate Stages of Aldehyde Oxidation. II Kinetics of the Interaction between Peracetic Acid and the Aldehydes. *J. Phys. Chem.* **1935**, *39*, 847−858.
(61) Hall, W. A.; Johnston, M. V. Oligomer Content of α-Pinene Secondary Organic Aerosol. *Aerosol Sci. Technol.* **2011**, *45*, 37−45.
(62) Lopez-Hilfiker, F. D.; Mohr, C.; Ehn, M.; Rubach, F.; Kleist, E.; Wildt, J.; Mentel, T. F.; Carrasquillo, A. J.; Daumit, K. E.; Hunter, J. F.; et al. Phase Partitioning and Volatility of Secondary Organic Aerosol Components formed from α-Pinene Ozonolysis and OH Oxidation: The Importance of Accretion Products and Other Low Volatility Compounds. *Atmos. Chem. Phys.* **2015**, *15*, 7765−7776.
(63) Müller, L.; Reinnig, C.; Warnke, J.; Hoffmann, T. Unambiguous Identification of Esters as Oligomers in Secondary Organic Aerosol formed from Cyclohexene and Cyclohexene/α-Pinene Ozonolysis. *Atmos. Chem. Phys.* **2008**, *8*, 1423−1433.
(64) Warscheid, B.; Hoffmann, T. On-line Measurements of α-Pinene Ozonolysis Products Using an Atmospheric Pressure Chemical Ionisation Ion-Trap Mass Spectrometer. *Atmos. Environ.* **2001**, *35*, 2927−2940.
(65) Zhang, X.; McVay, R. C.; Huang, D. D.; Dalleska, N. F.; Aumont, B.; Flagan, R. C.; Seinfeld, J. H. Formation and Evolution of Molecular Products in α-Pinene Secondary Organic Aerosol. *Proc. Natl. Acad. Sci. U. S. A.* **2015**, *112* (46), 14168−14173.
(66) Bailey, P. S. *Ozonation in Organic Chemistry. Vol. I: Olefinic Compounds*; Academic Press: New York, 1978.
(67) Hull, L. A.; Hisatsune, I. C.; Heicklen, J. Vapor-Phase Thermal Decomposition of Some Simple Ozonides. *J. Phys. Chem.* **1972**, *76*, 2659−2665.
(68) Tobias, H. J.; Ziemann, P. J. Thermal Desorption Mass Spectrometric Analysis of Organic Aerosol Formed from Reactions of 1-Tetradecene and O_3 in the Presence of Alcohols and Carboxylic Acids. *Environ. Sci. Technol.* **2000**, *34*, 2105−2115.
(69) Franzén, R.; Tanabe, K.; Morita, M. Ring-Chain Tautomerism of Chlorinated Hydroxyfuranones and Reaction with Nucleosides. *Chemosphere* **1999**, *38*, 973−980.
(70) Bell, R. P.; Higginson, W. C. E. The Catalyzed Dehydration of Acetaldehyde Hydrate, and the Effect of Structure on the Velocity of Protolytic Reactions. *Proc. R. Soc. London, Ser. A* **1949**, *197*, 141−159.
(71) Kurtén, T.; Tiusanen, K.; Roldin, P.; Rissanen, M.; Luy, J.; Boy, M.; Ehn, M.; Donahue, N. α-Pinene Autoxidation Products May Not Have Extremely Low Saturation Vapor Pressures Despite High O:C Ratios. *J. Phys. Chem. A* **2016**, *120*, 2569−2582.
(72) Rissanen, M. P.; Kurtén, T.; Sipil Sipilä, M.; Thornton, J. A.; Kangasluoma, J.; Sarnela, N.; Junninen, H.; Jørgensen, S.; Schallhart,

DOI: 10.1021/acsearthspacechem.8b00117
ACS Earth Space Chem. 2018, 2, 1196−1210

S.; Kajos, M. K.; et al. The Formation of Highly Oxidized Multifunctional Products in the Ozonolysis of Cyclohexene. *J. Am. Chem. Soc.* **2014**, *136*, 15596−15606.
(73) Clark, J.; English, A. M.; Hansen, J. C.; Francisco, J. S. Computational Study on the Existence of Organic Peroxy Radical-Water Complexes (RO_2•H_2O). *J. Phys. Chem. A* **2008**, *112*, 1587−1595.
(74) Prenni, A. J.; Petters, M. D.; Kreidenweis, S. M.; DeMott, P. J.; Ziemann, P. J. Cloud Droplet Activation of Secondary Organic Aerosol. *J. Geophys. Res.* **2007**, *112*, D10223.
(75) Ogata, Y.; Furuya, Y.; Maekawa, J.; Okano, K. Kinetics of the Acid-catalyzed Transformation of Peroxyacetic Acid to Acetyl Peroxide in Acetic Acid. *J. Am. Chem. Soc.* **1963**, *85*, 961−962.

DOI: 10.1021/acsearthspacechem.8b00117
ACS Earth Space Chem. 2018, 2, 1196−1210

Supporting Information

Functional Group Composition of Secondary Organic Aerosol Formed from Ozonolysis of α-Pinene Under High VOC and Autoxidation Conditions

Megan S. Claflin[†,‡], Jordan E. Krechmer[†,‡,§], Weiwei Hu[†,‡,‖], Jose L. Jimenez[†,‡], Paul J. Ziemann[†,‡,*]

Department of Chemistry and Biochemistry, and Cooperative Institute for Research in Environmental Sciences (CIRES), Boulder, Colorado 80309

† Cooperative Institute for Research in Environmental Sciences (CIRES), Boulder, Colorado 80309, United States

‡ Department of Chemistry and Biochemistry, University of Colorado, Boulder, Colorado 80309, United States

§ Now at Aerodyne Research, Inc., Billerica, MA, USA 01821

‖ Now at State Key Laboratory of Organic Geochemistry and Guangdong Key Laboratory of Environment Protection and Resources Utilization, Guangzhou Institute of Geochemistry, Chinese Academy of Sciences, Guangzhou 510640, China

Abstract. Bar graph of measured and modeled functional group compositions (Figure S1). Reported functional group compositions, SOA properties, and yields from individual experiments conducted for the High-VOC (Table S1, S2) and Low-VOC (Table S3, S4) systems.

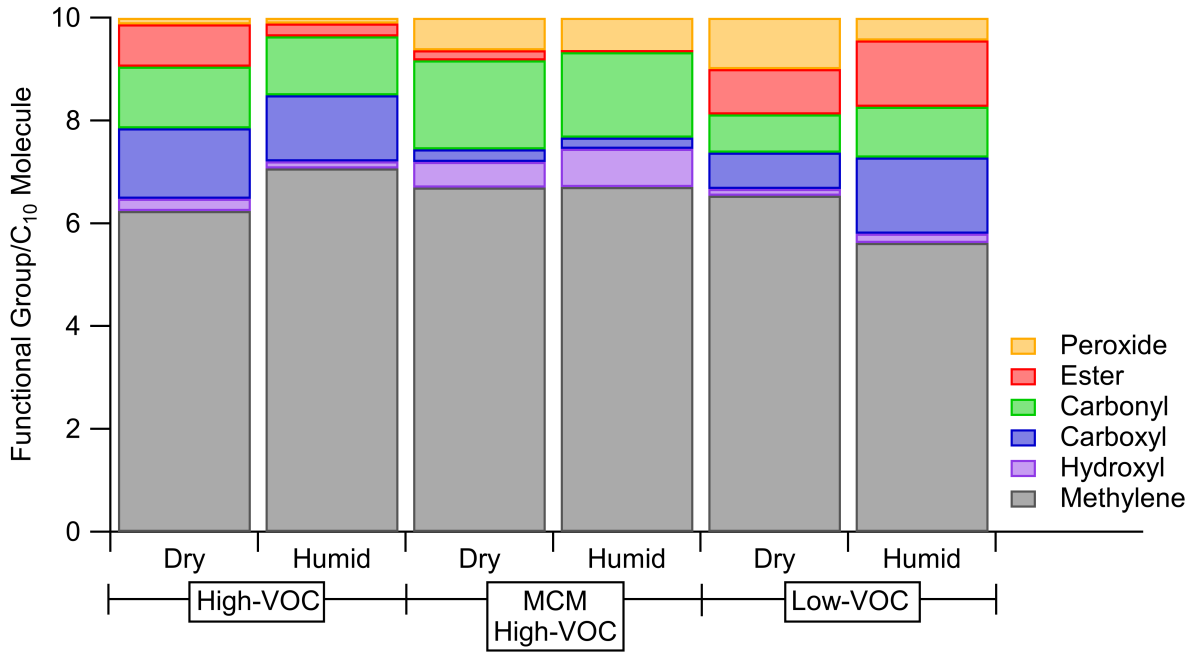

Figure S1. Results of measurements and MCM modeling of the functional group composition of SOA formed from reactions of α-pinene with O_3 under a variety of conditions.

Table S1. Functional group composition of SOA formed from reactions of α-pinene with O_3 under High-VOC conditions.

	High-VOC		
	Dry	Humid 50%	Humid 85%
Functional Group	Functional Group/C_{10} Molecule		
Peroxide [HCOOH]	0.13	0.09	0.12
Ester [O=COR]	0.82	0.27	0.23
Carbonyl [C=O]	1.20	0.95	1.34
Carboxyl [O=COH]	1.37	1.22	1.33
Hydroxyl [HCOH]	0.24	0.06	0.21
Total FG	3.76	2.59	3.22
Methylene [CH_2]	6.24	7.41	6.78

Table S2. Chemical properties and yields of SOA formed from reactions of α-pinene with O_3 under High-VOC conditions.

	High-VOC		
	Dry	Humid	Humid
		50%	85%
O/C	0.61	0.42	0.49
H/C	1.46	1.63	1.55
MW[a]	232	203	214
C* ($\mu g\ m^{-3}$)	1	20	2
Density[b] (g/mL)	1.38	1.20	1.27
SOA Mass Yield[c]	0.78	0.41	0.48
SOA Molar Yield[d]	0.45	0.27	0.31

[a] Average MW (g mol^{-1}) per C_{10} molecule calculated using the FG data.
[b] Density of the SOA calculated using the methods of Kuwata et al.[1]
[c] SOA mass yield calculated by combining filter mass data with SMPS volume data to correct for wall loss.
[d] SOA molar yield calculated using the SOA mass yield (c) and reported average MW of products.

Table S3. Functional group composition of SOA formed from reactions of α-pinene with O_3 under Low-VOC conditions.

	Low-VOC						
	Dry I	Dry II	Dry III	Dry IV	Humid I	Humid II	Humid III
					65%		
Functional Group	Functional Group/C_{10} Molecule						
Peroxide [HCOOH]	1.00	1.00	1.00	1.01	0.64	0.36	0.32
Ester [O=COR]	0.77	0.87	1.01	0.89	1.37	1.19	1.32
Carbonyl [C=O]	0.73	0.67	0.64	0.91	1.21	0.71	1.06
Carboxyl [O=COH]	0.69	0.70	0.74	0.71	2.01	1.18	1.24
Hydroxyl [HCOH]	0.13	0.18	0.08	0.13	0.13	0.15	0.26
Total FG	3.32	3.43	3.47	3.65	5.36	3.59	4.20
Methylene [CH_2]	6.68	6.57	6.53	6.35	4.64	6.41	5.80

Table S4. Chemical properties and yields of SOA formed from reactions of α-pinene with O_3 under Low-VOC conditions.

	Low-VOC						
	Dry I	Dry II	Dry III	Dry IV	Humid I	Humid II	Humid III
						65%	
O/C	0.58	0.60	0.61 0.58[a]	0.63	0.94	0.63 0.58[a]	0.71 0.50[a]
H/C	1.63	1.62	1.60 1.60[a]	1.57	1.28	1.50 1.70[a]	1.40 1.67[a]
MW[b]	229	232	236	236	283	236	247
C* ($\mu g\ m^{-3}$)	30	20	20	10	2×10^{-5}	1	0.1
Density[c] (g/mL)	1.30	1.32	1.34	1.35	1.64	1.38	1.46
SOA Mass Yield[d]	0.26	0.20	0.23	0.20	0.25	0.26	0.21
SOA Molar Yield[e]	0.15	0.12	0.13	0.12	0.12	0.15	0.12

[a] O/C and H/C ratios measured by online HR-ToF-AMS.
[b] Average MW ($g\ mol^{-1}$) per C_{10} molecule calculated using the FG data.
[c] Density of the SOA calculated using the methods of Kuwata et al.[1]
[d] SOA mass yield calculated by combining filter mass data with SMPS volume data to correct for wall loss.
[e] SOA molar yield calculated using the SOA mass yield (d) and reported average MW of products.

REFERENCES

(1) Kuwata, M.; Zorn, S. R.; Martin, S. T. Using Elemental Ratios to Predict the Density of Organic Material Composed of Carbon, Hydrogen, and Oxygen. *Environ. Sci. Technol.* **2012**, 46, 787–794.